AD-A065 439 CALIFORNIA INST OF TECH PASADENA DIV OF ENGINEERING--ETC F/G 20/11
DISCONTINUOUS DEFORMATION GRADIENTS NEAR THE TIP OF A CRACK IN --ETC(U)
JAN 79 J K KNOWLES, E STERNBERG N00014-75-C-0196

UNCLASSIFIED TR-40 NL

1 OF 1
AD A065439

END
DATE FILMED
4-79
DDC

OFFICE OF NAVAL RESEARCH
CONTRACT N00014-75-C-0196

(12) LEVEL II

TECHNICAL REPORT NO. 40

DISCONTINUOUS DEFORMATION GRADIENTS NEAR THE TIP OF A CRACK IN FINITE ANTI-PLANE SHEAR: AN EXAMPLE

BY
J. K. KNOWLES AND ELI STERNBERG

DIVISION OF ENGINEERING AND APPLIED SCIENCE
CALIFORNIA INSTITUTE OF TECHNOLOGY
PASADENA, CALIFORNIA

JANUARY, 1979

Office of Naval Research
Contract N00014-75-C-0196
(15)

Technical Report No. 40

(9) Research rept.,

(6)

Discontinuous deformation gradients near the tip of a crack in finite anti-plane shear: an example,

(10) by
James K. Knowles Eli Sternberg

(14) TR-40

Division of Engineering and Applied Science
California Institute of Technology
Pasadena, California 91125

(12) 64 pp.

(11) Jan 1979

Discontinuous deformation gradients near the tip of a crack in finite anti-plane shear: an example*

by

J. K. Knowles and Eli Sternberg

California Institute of Technology

Summary

This investigation aims at the elastostatic field near the edges (tips) of a plane crack of finite width in an all-around infinite body, which — at infinity — is subjected to a state of simple shear parallel to the crack faces. The analysis is carried out within the fully nonlinear equilibrium theory of homogeneous and isotropic, incompressible elastic solids. Further, the particular constitutive law employed here gives rise to a loss of ellipticity of the governing displacement equation of equilibrium in the presence of sufficiently severe anti-plane shear deformations.

The study reported in this paper is asymptotic in the sense that the actual crack is replaced by a semi-infinite one, while the far field is required to match the elastostatic field predicted near the crack tips by the linearized theory for a crack of finite width. The ensuing global boundary-value problem thus characterizes the local state of affairs in the vicinity of a crack-tip, provided the amount of shear applied at infinity is suitably small.

---

*The results communicated in this paper were obtained in the course of an investigation supported by Contract N00014-75-C-0196 with the Office of Naval Research in Washington, D. C.

An explicit exact solution to this problem, which is deduced with the aid of the hodograph method, exhibits finite shear stresses at the tips of the crack, but involves two symmetrically located lines of displacement-gradient and stress discontinuity issuing from each crack-tip.

Introduction

In a number of investigations conducted during the past few years we have explored two distinct types of inherently nonlinear singular problems in finite elastostatics. The first of these categories pertains to geometrically induced point or line singularities, such as those arising in connection with crack and punch problems, for which the linearized theory of ealsticity – in conflict with its underlying approximative assumptions – predicts locally unbounded deformation gradients. The second category, which has no counterpart in linear elastostatics, concerns the emergence of lines or surfaces across which the deformation gradients suffer finite jump discontinuities. This kind of singular behavior becomes possible only if the elastic material is such as to admit a failure of ellipticity in the corresponding displacement equations of equilibrium at sufficiently severe deformations.

The results obtained in these investigations aresummarized in a comprehensive survey [1], which also contains references to the related background literature[1]. The present paper extends, and combines strands from, both strings of studies alluded to above. It deals with the elastostatic field near the tip of a crack under conditions of anti-plane shear in a constitutive setting within the fully nonlinear equilibrium theory that

[1] In this paper we shall cite explicitly only previous work that is of immediate relevance to our current purpose.

leads to a loss of ellipticity and the concomitant appearance of lines of deformation-gradient discontinuity ("elastostatic shocks") in the vicinity of the crack-tips.

The particular problem treated here is suggested by and complements an asymptotic study reported in [2]. We consider an all-around infinite — homogeneous and isotropic — incompressible elastic body with a plane crack of constant width and infinite length. At infinity the body is subjected to a state of simple shear, parallel to the faces of the crack. In [2] the deformations and stresses ensuing near the tips (edges) of the crack were analyzed for a class of such materials whose elastic potential (strain-energy density) is completely determined by the shear-stress response to a simple-shear deformation. Moreover, the analysis carried out in [2] was confined to circumstances in which the induced shear stress is a steadily increasing function of the amount of simple shear applied. In this instance the displacement equations of equilibrium are found to be elliptic at all field points and at every solution corresponding to anti-plane shear. In contrast, ellipticity is lost at severe enough anti-plane shear deformations if the response curve in simple shear undergoes at least one reversal in slope.

The case in which the response curve in simple shear has a positive slope throughout but rises monotonically to a <u>finite</u> shear stress — as the amount of shear grows beyond bounds — thus signals an impending breakdown of ellipticity, which would occur if the stress were to increase steadily to a maximum value at a <u>finite</u> amount of shear and thereafter declined monotonically. This troublesome transition case is still fully discussed in [2] with the aid of the hodograph method and on the basis of an asymptotic scheme in which the crack of finite width is replaced by one

of semi-infinite width, while the far field is required to match the elastostatic field near the crack-tip predicted by the solution to the original problem according to the linear theory.

The results deduced in [2] for the limiting elliptic case described above, though of unlimited smoothness in the interior of the body, display certain features that suggest the emergence of discontinuities in the deformation gradients once ellipticity is lost. In order to explore this eventuality by means of a pilot example we presuppose here a specific response curve in simple shear that rises linearly to a maximum shear stress and then declines steadily as the amount of shear increases. The special constitutive assumption thus introduced enables us to establish on the basis of the hodograph method an explicit exact solution to the crack problem under present consideration. The solution thus obtained involves two lines of displacement-gradient and stress discontinuity that are symmetrically located with respect to the axis of the crack, issue from the crack-tip, and terminate in the interior of the body.

1. Preliminaries. Finite anti-plane shear for incompressible elastic solids. Formulation of crack problem.

In this section we cite from [2] certain prerequisites needed here. Suppose the interior of a body occupies an open region $\mathcal{R}$ in an undeformed configuration and consider a deformation

$$\underset{\sim}{y} = \underset{\sim}{y}(\underset{\sim}{x}) = \underset{\sim}{x} + \underset{\sim}{u}(\underset{\sim}{x}) \quad \text{for all } \underset{\sim}{x} \in \mathcal{R} \tag{1.1}$$

that maps $\mathcal{R}$ onto its deformation image $\mathcal{R}^*$. Here $\underset{\sim}{x}$ is the position vector of a material point in $\mathcal{R}$, $\underset{\sim}{y}(\underset{\sim}{x})$ its position vector in $\mathcal{R}^*$, and $\underset{\sim}{u}(\underset{\sim}{x})$

[1] Boldface letters are used to denote vectors or tensors.

its displacement vector. We assume the mapping (1.1) to be suitably smooth and invertible. Let

$$\underset{\sim}{F} = \nabla \underset{\sim}{y} = \underset{\sim}{1} + \nabla \underset{\sim}{u} \text{ on } \mathcal{R} \ , \tag{1.2}$$

[1]

so that $\underset{\sim}{F}(\underset{\sim}{x})$ is the deformation-gradient tensor at $\underset{\sim}{x}$. For an incompressible medium the deformation must be locally volume preserving and thus

$$J = \det \underset{\sim}{F} = 1 \text{ on } \mathcal{R} \tag{1.3}$$

The left deformation tensor associated with (1.1) is given by

$$\underset{\sim}{G} = \underset{\sim}{F}\underset{\sim}{F}^{T} \tag{1.4}$$

[2]

and has the fundamental scalar invariants

$$I_1 = \operatorname{tr} \underset{\sim}{G} \ , \ I_2 = \tfrac{1}{2}[\operatorname{tr} \underset{\sim}{G})^2 - \operatorname{tr}(\underset{\sim}{G}^2)] \ , \ I_3 = \det \underset{\sim}{G} = J^2 = 1 \ . \tag{1.5}$$

Next, let $\underset{\sim}{\tau}$ be the actual (Cauchy) stress tensor field on $\mathcal{R}^*$ and $\underset{\sim}{\sigma}$ the corresponding nominal (Piola) stress field on $\mathcal{R}$, whence

$$\underset{\sim}{\tau} = \underset{\sim}{\sigma}\underset{\sim}{F}^{T} \ , \ \underset{\sim}{\sigma} = \underset{\sim}{\tau}(\underset{\sim}{F}^{T})^{-1} \ . \tag{1.6}$$

[3]

The balance of linear momentum, in the absence of body forces, leads to the equilibrium equations

$$\operatorname{div} \underset{\sim}{\tau} = \underset{\sim}{0} \text{ on } \mathcal{R}^* \text{ or } \operatorname{div} \underset{\sim}{\sigma} = \underset{\sim}{0} \text{ on } \mathcal{R} \ . \tag{1.7}$$

Suppose further the incompressible medium at hand is a homogeneous, isotropic, elastic solid that possesses a strain-energy density W per unit undeformed volume. In this instance $W = W(I_1, I_2)$ and the

---

[1] We write $\underset{\sim}{1}$ for the idem-tensor.

[2] The superscript T indicates transposition.

[3] If $\underset{\sim}{A}$ is a nonsingular tensor, $\underset{\sim}{A}^{-1}$ stands for its inverse.

appropriate constitutive law takes the equivalent alternative forms:

$$\underset{\sim}{\tau} = 2\left[\frac{\partial W}{\partial I_1}\underset{\sim}{G} + \frac{\partial W}{\partial I_2}(I_1\underset{\sim}{1} - \underset{\sim}{G})\underset{\sim}{G}\right] - p\underset{\sim}{1} \ , \tag{1.8}$$

$$\underset{\sim}{\sigma} = 2\left[\frac{\partial W}{\partial I_1}\underset{\sim}{F} + \frac{\partial W}{\partial I_2}(I_1\underset{\sim}{1} - \underset{\sim}{G})\underset{\sim}{F}\right] - p(\underset{\sim}{F}^T)^{-1} \ , \tag{1.9}$$

where p is the arbitrary hydrostatic pressure required to accommodate the kinematical constraint (1.3). The stress-deformation relation (1.8) assures the symmetry of $\underset{\sim}{\tau}$, but $\underset{\sim}{\sigma}$ is in general not symmetric.

If S is a surface in $\mathcal{R}$ and S^* its deformation image in $\mathcal{R}^*$, one has

$$\underset{\sim}{\tau}\underset{\sim}{n}^* = \underset{\sim}{0} \text{ on } S^* \text{ if and only if } \underset{\sim}{\sigma}\underset{\sim}{n} = \underset{\sim}{0} \text{ on } S \ , \tag{1.10}$$

where $\underset{\sim}{n}$ and $\underset{\sim}{n}^*$ are the respective unit normal vectors of S and S^*. Thus, in particular, a portion of the boundary of $\mathcal{R}^*$ is free of actual tractions provided the nominal traction vanishes on its antecedent within the boundary $\mathcal{R}$. Further the actual traction $\underset{\sim}{t} = \underset{\sim}{\tau}\underset{\sim}{n}^*$ is found to be continuous across S^* if and only if the nominal traction $\underset{\sim}{s} = \underset{\sim}{\sigma}\underset{\sim}{n}$ is continuous across S.

With a view toward the crack problem that constitutes our objective we now assume that $\mathcal{R}$ is the exterior of a plane infinite strip of width $2c$. Further, we introduce rectangular cartesian coordinates (x_1, x_2, x_3) in such a way that this strip, which represents the crack, lies in the plane $x_2 = 0$, the x_3-axis being parallel to the edges of the crack and the origin midway between the edges. Figure 1 shows the cross-section $\mathcal{S}$ of $\mathcal{R}$ in the plane $x_3 = 0$. Evidently, the plane domain $\mathcal{S}$ is the exterior of the line segment $x_2 = 0$, $-c \le x_1 \le c$ in the (x_1, x_2)-plane. We confine our

attention now to the case in which the body is subjected at infinity to a simple shear parallel to the crack faces[1]. The displacement components u_i are thus required to satisfy[2]

$$u_\alpha = o(1)\ ,\ u_3 = kx_2 + o(1) \quad \text{as} \quad x_\alpha x_\alpha \to \infty \ (-\infty < x_3 < \infty)\ , \tag{1.11}$$

in which the positive constant k is the amount of the applied shear. Moreover, the deformed faces of the crack are taken to remain free of actual tractions. In view of (1.10), this assumption yields the boundary conditions

$$\sigma_{i2}(x_1, 0\pm, x_3) = 0 \ (-c < x_1 < c,\ -\infty < x_3 < \infty) \tag{1.12}$$

for the components σ_{ij} of the nominal stress field. If $\mathcal{R}$ is understood to be the particular domain just defined, the crack problem to be considered accordingly consists in finding a deformation (1.1) obeying the incompressibility condition (1.3), as well as a hydrostatic pressure field, such that the displacements satisfy (1.11), while the associated nominal stress field (1.9) satisfies the equilibrium equation (1.7) and meets the boundary conditions (1.12).

At this stage we restrict ourselves to the class of incompressible elastic solids for which W is independent of the second deformation invariant and set

$$W = W(I_1) \quad \text{for all} \quad I_1 \geq 3\ ,\ W(3) = 0\ . \tag{1.13}$$[3]

---

[1] This loading case is known as "Mode III" in the terminology of fracture mechanics.

[2] Latin and Greek subscripts have the ranges (1, 2, 3) and (1, 2), respectively. Summation over repeated subscripts is taken for granted.

[3] It is easily seen from (1.4), (1.5) that $I_1 = 3$ at the undeformed state and that otherwise $I_1 > 3$.

Such a solid has a shear modulus at infinitesimal deformations given by

$$\mu = 2W'(3) \tag{1.14}$$[1]

and conforms to the Baker-Ericksen inequality, provided

$$W'(I_1) > 0 \quad \text{for} \quad I_1 > 3 \ . \tag{1.15}$$

In particular, for a NeoHookean material,

$$W(I_1) = \frac{\mu}{2}(I_1 - 3) \ . \tag{1.16}$$

For materials governed by the strain-energy density (1.13) the foregoing crack problem is consistent with the assumption that the ensuing deformation throughout $\mathcal{R}$ is one of anti-plane shear parallel to the faces of the crack:

$$u_\alpha = 0 \ , \ u_3 = u(x_1, x_2) \ \text{ on } \ \mathcal{R} \ . \tag{1.17}$$

Indeed, as shown in [2], (1.17) enables one to reduce the original three-dimensional problem to the following subsidiary two-dimensional boundary value problem for the unknown out-of-plane displacement u on the cross-sectional domain $\mathcal{D}$:

$$[W'(I_1)u_{,\alpha}]_{,\alpha} = 0 \ \text{ on } \ \mathcal{D} \ , \tag{1.18}$$[2]

with

$$I_1 = 3 + |\nabla u|^2 \ , \ |\nabla u|^2 = u_{,\alpha}u_{,\alpha} \ ; \tag{1.19}$$

---

[1] Here and in what follows $W'(I_1)$ stands for the derivative of W with respect to its argument I_1.

[2] Subscripts preceded by a comma indicate partial differentiation with respect to the corresponding material cartesian coordinate.

$$u(x_1, x_2) = kx_2 + o(1) \quad \text{as} \quad x_\alpha x_\alpha \to \infty \ , \tag{1.20}$$

$$u_{,2}(x_1, 0\pm) = 0 \quad (-c < x_1 < c) \ . \tag{1.21}$$

The hydrostatic pressure $p = 2W'(I_1)$ on $\mathcal{D}$ in the present instance and (1.17), (1.13) together with (1.8), (1.9) yield the stress-displacement relations

$$\tau_{3\alpha} = \tau_{\alpha 3} = \sigma_{3\alpha} = \sigma_{\alpha 3} = 2W'(I_1)u_{,\alpha} \ , \tag{1.22}$$

$$\tau_{\alpha\beta} = \sigma_{\alpha\beta} = \sigma_{33} = 0 \ , \ \tau_{33} = 2W'(I_1)|\nabla u|^2 \ , \tag{1.23}$$

with I_1 supplied by (1.19).

We now specify the smoothness demanded of the solution u to the boundary-value problem characterized by (1.18), (1.19), (1.20), (1.21). In this connection we suppose that W has a continuous first derivative and at least a piecewise continuous second derivative on its interval of definition $[3, \infty)$. Further, we restrict u to be continuous and to possess piecewise continuous first and second partial derivatives on $\mathcal{D}$; in addition, u is to be bounded on every finite sub-domain of $\mathcal{D}$. Thus, in particular, u must remain bounded within any circle of finite radius centered at either crack-tip. Next, the limits $\nabla u(x_1, 0\pm)$ are to exist and be continuous for $-c < x_1 < c$. Observe that the preceding smoothness restrictions allow for the possibility of finite jump discontinuities in ∇u — and hence also in the stresses τ_{3i} — across curves in $\mathcal{D}$. If $\mathcal{L}$ is such a curve, however, we stipulate that $W'(I_1)\partial u/\partial n$ be continuous across $\mathcal{L}$, provided $\underset{\sim}{n}$ is the unit normal vector of $\mathcal{L}$ and $\partial u/\partial n = \nabla u \cdot \underset{\sim}{n}$. Let $\underset{\sim}{s} = \underset{\sim\sim}{\sigma}\underset{\sim}{n}$, so that $\underset{\sim}{s}$ is the nominal traction vector along $\mathcal{L}$. One draws from (1.22), (1.23) that

$$s_\alpha = 0 \ , \ s_3 \equiv s = 2W'(I_1)\frac{\partial u}{\partial n} \ \text{ on } \ \mathscr{S} \ . \tag{1.24}$$

The foregoing continuity condition therefore assures the continuity of the Piola tractions across the cylindrical surface whose trace upon $\mathscr{B}$ is $\mathscr{S}$. Consequently[1], the Cauchy tractions are continuous across the deformation image of this surface. The continuity of both the nominal and the actual tractions, in turn, is a necessary equilibrium requirement.

If the boundary conditions (1.21) are deleted and $\mathscr{B}$ is momentarily taken to be the entire (x_1, x_2)-plane, i.e. in the absence of a crack, the differential equation (1.18), subject to the condition (1.20) at infinity, clearly admits the elementary solution

$$u(x_1, x_2) = kx_2 \ \text{ for all } \ (x_1, x_2) \in \mathscr{B} \ , \tag{1.25}$$

which corresponds to an undisturbed homogeneous field of simple shear of amount k. Also, (1.22), (1.23) now furnish

$$\tau_{23} = \tau_{32} = \tau(k) = 2W'(3 + k^2)k \ , \ \tau_{33} = \tau(k)k \ \ (0 \le k < \infty) \ , \tag{1.26}$$

while all remaining components of actual stress vanish identically. We shall henceforth refer to the graph of $\tau(k)$ $(0 \le k < \infty)$ as the response curve in simple shear. For the special case of the Neo-Hookean solid, with the strain-energy density (1.16), $\tau(k) = \mu k$ and this response curve is a straight line. Bearing (1.13) and (1.25) in mind one sees at once that the response curve in simple shear, in turn, completely determines the strain-energy density for an incompressible elastic solid of the type under consideration:

---

[1] See the remarks following (1.10).

$$W(I_1) = \int_0^{\sqrt{I_1 - 3}} \tau(k)\,dk \qquad (3 \le I_1 < \infty) \ . \tag{1.27}$$

Finally, we observe in connection with (1.26) that the Baker-Ericksen inequality (1.15) is equivalent to the obvious physical requirement that the "modulus of shear" $2W'(3+k^2)$ be positive at <u>all</u> values of k.

When (1.15) is in force, one confirms readily that the quasilinear second-order partial differential equation (1.18) is <u>elliptic</u> at a solution u and at a point (x_1, x_2) if and only if

$$W'(3+k^2) + 2k^2 W''(3+k^2) > 0 \ , \ k = |\nabla u(x_1, x_2)| \ . \tag{1.28}$$

On the other hand, as is clear from (1.26), this inequality is satisfied if and only if $\tau'(k) > 0$, so that the response curve in simple shear has a positive slope at an amount of shear equal to the magnitude of the local displacement gradient $\nabla u(x_1, x_2)$. It follows that (1.18) cannot admit a loss of ellipticity if the response curve in simple shear represents a strictly increasing function[1].

We conclude this section with two examples of incompressible elastic solids within the class of such solids subsumed in (1.13). The first of these concerns the subclass of "power-law materials" introduced in [2], which is governed by the elastic potential

$$W(I_1) = \frac{\mu}{2b}\left\{\left[1 + \frac{b}{n}(I_1 - 3)\right]^n - 1\right\} \qquad (3 \le I_1 < \infty) \ , \tag{1.29}$$

where μ, n, and b are positive material constants. In view of (1.26),

[1] If such is the case, we shall — in the present context — call the elastic solid an "elliptic material".

the response curve in simple shear here is characterized by

$$\tau(k) = \mu\left[1 + \frac{b}{n}k^2\right]^{n-1} k \quad (0 \le k < \infty) \ , \tag{1.30}$$

μ being the shear modulus at infinitesimal deformations. Figure 2 illustrates the response in shear for various values of the "hardening parameter" n. A power-law material hardens or softens in simple shear according as $n > 1$ or $n < 1$. The case $n = 1$ corresponds to the special case of the Neo-Hookean solid. For $n \ge 1/2$, $\tau(k)$ is monotone strictly increasing; further, if $n > 1/2$, $\tau(k) \to \infty$ as $k \to \infty$, while $\tau(k)$ tends to the finite "ultimate shear stress" $\mu/\sqrt{2b}$ as $k \to \infty$ if $n = 1/2$. On the other hand, in the range $0 < n < 1/2$, $\tau(k)$ rises steadily to a maximum at $k = k_0 = \sqrt{n/b(1-2n)}$ and thereafter decreases steadily to zero as $k \to \infty$. Thus, all solutions of the displacement equation of equilibrium (1.18) are bound to be elliptic everywhere when $n \ge 1/2$. In contrast, when $n < 1/2$, a solution of (1.18) that involves displacement gradients of a magnitude exceeding k_0 at some point entails a local loss of ellipticity. The transition case $n = 1/2$ is evidently the limiting elliptic case.

We turn finally to a second, much more specialized, ideal incompressible elastic solid that serves as a basis of the present pilot study. The elastic potential defining this material is given by

$$\left.\begin{aligned} W(I_1) &= \frac{\mu}{2}(I_1 - 3) \quad (3 \le I_1 \le 4) \ , \\ W(I_1) &= -\frac{3\mu}{2} + 2\mu(I_1 - 3)^{1/4} \quad (4 \le I_1 < \infty) \ , \end{aligned}\right\} \tag{1.31}$$

in which the positive constant μ is again the shear modulus at infinitesimal deformations. The corresponding response in simple shear obeys

$$\tau(k) = \mu k \quad (0 \le k \le 1) \ , \ \tau(k) = \mu k^{-1/2} \quad (1 \le k < \infty) \ . \tag{1.32}$$

Figure 3 displays the graph associated with (1.32). Note that the response in the present instance is linear (Neo-Hookean) up to a shear of amount $k = 1$, whereas $\tau(k)$ is monotone decreasing for $1 \le k < \infty$ and $\tau(k) \to 0$ as $k \to \infty$. Clearly, the location of the peak of the response curve at $k = 1$ is a matter of convenience only[1]. Equation (1.18) at present suffers a loss of ellipticity at a solution u and a point (x_1, x_2) if $|\nabla u(x_1, x_2)| > 1$. Observe that while the elastic potential (1.29) has continuous derivatives of all orders, W in (1.31) is merely once continuously differentiable on its interval of definition $[3, \infty)$; the second derivative of this elastic potential has a finite jump discontinuity at $I_1 = 4$.

2. <u>The small-scale nonlinear crack problem. Hodograph transformation</u>.

Upon a linearization with respect to $|\nabla u|$, the differential equation (1.18) reduces to Laplace's equation and (1.22), (1.23) pass over into the stress-displacement relations appropriate to infinitesimal anti-plane shear deformations. The boundary-value problem for u governed by (1.18), (1.20), (1.21) under such a linearization becomes identical with that characterizing the analogous crack problem in linear elastostatics. This linear boundary-value problem, in turn, is mathematically identical with the one governing the velocity potential of a steady irrotational flow of an inviscid incompressible fluid past a flat plate of width $2c$ at a right angle of attach.

If (r, θ) are polar coordinates at the right-hand crack-tip (see

---

[1] The case in which this peak occurs at $k = k_0$ $(k_0 > 0)$ is reducible to the case $k_0 = 1$ by means of an obvious re-scaling.

Figure 1) the asymptotic behavior, as $r \to 0$, of the displacement $\mathring{u}$ and of the shear stresses $\mathring{\tau}_{3\alpha}$ belonging to the well-known solution of the linearized crack problem is given by

$$\left.\begin{aligned} \mathring{u} &\sim k(2cr)^{1/2}\sin\tfrac{\theta}{2} \ , \\ \mathring{\tau}_{31} &= \mu\mathring{u}_{,1} \sim -\mu kc(2cr)^{-1/2}\sin\tfrac{\theta}{2} \ , \\ \mathring{\tau}_{32} &= \mu\mathring{u}_{,2} \sim \mu kc(2cr)^{-1/2}\cos\tfrac{\theta}{2} \ . \end{aligned}\right\} (2.1)^1$$

The normal stress $\mathring{\tau}_{33}$ vanishes identically according to the linear theory.

For our purposes it is essential to remark that for the Neo-Hookean elastic potential (1.16) the non-linear crack problem (1.18)-(1.21) specializes exactly (rather than merely by linearization) to the linear problem of which $\mathring{u}$ is the solution. Further, for the Neo-Hookean material $\tau_{3\alpha}$ coincides with $\mathring{\tau}_{3\alpha}$, but τ_{33} now no longer vanishes. In fact, for this special material one finds from (1.23) and (2.1) that

$$\tau_{33} = \mu|\nabla u|^2 \sim \frac{\mu k^2 c}{2r} \quad \text{as} \quad r \to 0 \ . \tag{2.2}$$

According to (2.1), the stresses $\mathring{\tau}_{3\alpha}$ – and hence also the corresponding infinitesimal shearing strains – become unbounded as $r \to 0$. Consequently the solution of the crack problem based on linear elastostatics cannot be valid arbitrarily close to the crack-tips. It is plausible to assume, however, that for a small enough amount of shear k at infinity, the asymptotic

---

[1] See, for example, I. N. Sneddon and M. Lowengrub [3], Section 2.6. Note that the right member in the first of (2.1) is an exact solution of Laplace's equation that has a vanishing normal derivative along $r>0$, $\theta = \pm\pi$.

estimates (2.1) are realistic within a suitably small circular annulus centered at the right crack-tip (see Figure 4). On the other hand, the deformations and stresses in the interior of the circular disk surrounded by this annulus – except possibly at the tip of the crack, where they may not be defined – are governed by the finite theory and must match the near field predicted by (2.1) as the inner boundary of the annulus is traversed. A magnification of this local state of affairs, which in the context of plasticity theory[1] is known as "small-scale yielding", leads to the following global boundary-value problem for the domain $\mathfrak{D}$ (see Figure 4) comprising all points exterior to the half-axis $-\infty < x_1 \leq 0$, $x_2 = 0$, which may now be regarded as representing a crack of semi-infinite width. If (r, θ) are at present polar coordinates at the origin, so that

$$x_1 = r\cos\theta\ ,\ x_2 = r\sin\theta\ \ (0 \leq r < \infty,\ -\pi \leq \theta < \pi)\ , \tag{2.3}$$

the ensuing "small-scale nonlinear crack problem" consists in finding a solution of the partial differential equation (1.18) on $\mathfrak{D}$, subject to the boundary conditions

$$u_{,2}(x_1, 0\pm) = 0 \quad (-\infty < x_1 < 0) \tag{2.4}$$

and the matching conditions

$$\left.\begin{aligned} u &\sim k(2cr)^{1/2}\sin\tfrac{\theta}{2}\ , \\ u_{,1} &\sim -kc(2cr)^{-1/2}\sin\tfrac{\theta}{2}\ ,\ u_{,2} \sim kc(2cr)^{-1/2}\cos\tfrac{\theta}{2} \\ &\text{as } r \to \infty\ \ (-\pi \leq \theta < \pi)\ . \end{aligned}\right\} \tag{2.5}$$

[1] See Rice [4].

Furthermore, the desired solution u is to satisfy relaxed regularity requirements strictly analogous to those imposed in connection with the original nonlinear crack problem[1].

When referred to the dimensionless variables

$$\bar{x}_\alpha = x_\alpha / ck^2 \ , \ \bar{r} = r/ck^2 \ , \ \bar{u} = u/ck^2 \ , \tag{2.6}$$

the boundary-value problem (1.18), (2.4), (2.5) assumes the following non-dimensional form in which k does not appear explicitly:

$$[W'(3 + |\bar{\nabla}\bar{u}|^2)\bar{u}_{,\alpha}]_{,\alpha} = 0 \quad \text{on} \quad \mathfrak{D} \tag{2.7}$$

[2]

$$\bar{u}_{,2}(\bar{x}_1, 0\pm) = 0 \qquad (-\infty < \bar{x}_1 < 0) \ ; \tag{2.8}$$

$$\left.\begin{aligned} \bar{u} &\sim (2\bar{r})^{1/2} \sin\frac{\theta}{2} \ , \\ \bar{u}_{,1} &\sim (2\bar{r})^{-1/2} \sin\frac{\theta}{2} \ , \quad \bar{u}_{,2} \sim (2\bar{r})^{-1/2} \cos\frac{\theta}{2} \\ &\text{as } r \to \infty \quad (-\pi \le \theta < \pi) \ . \end{aligned}\right\} \tag{2.9}$$

The foregoing small-scale nonlinear crack problem was solved in [2] by means of the hodograph method for the limiting elliptic case $n = 1/2$ of a power-law material with the elastic potential given by (1.29). Reverting to the general class of incompressible elastic materials governed by $W = W(I_1)$, we merely sketch here a formal approach to the problem based on the hodograph method and refer to [2] for a detailed exposition

---

[1] See the regularity conditions listed after (1.23).

[2] Subscripts preceded by a comma are now understood to indicate partial differentiation with respect to the dimensionless material coordinates $\bar{x}_\alpha$ and $\bar{\nabla}$ stands for the gradient operator with the components $\partial/\partial\bar{x}_\alpha$.

of this scheme.

The underlying hodograph transformation is the mapping

$$\xi_\alpha = \bar{u}_{,\alpha}(\bar{x}_1, \bar{x}_2) \quad \text{for all} \quad (\bar{x}_1, \bar{x}_2) \in \mathfrak{D} \tag{2.10}$$

from the physical $(\bar{x}_1, \bar{x}_2)$-plane into the hodograph plane spanned by the rectangular cartesian coordinates (ξ_1, ξ_2). We shall limit our attention temporarily to a material satisfying the ellipticity condition $\tau'(k) > 0$ $(0 \le k < \infty)$. Further, we take for granted that (2.10) is a one-to-one continuously differentiable mapping of $\mathfrak{D}$ onto its as yet undetermined image Δ in the hodograph plane. The latter assumption entitles us to introduce, in place of $\bar{u}$, its Legendre transform $\bar{U}$ as a new dependent variable:

$$\bar{U}(\xi_1, \xi_2) = \bar{x}_\beta \bar{u}_{,\beta}(\bar{x}_1, \bar{x}_2) - \bar{u}(\bar{x}_1, \bar{x}_2) = \bar{x}_\beta \xi_\beta - \bar{u}(\bar{x}_1, \bar{x}_2) \ . \tag{2.11}$$

From (2.10), (2.11) follow

$$\bar{x}_\alpha = \frac{\partial}{\partial \xi_\alpha} \bar{U}(\xi_1, \xi_2) \quad \text{on} \quad \Delta \ , \tag{2.12}$$

$$\bar{u}(\bar{x}_1, \bar{x}_2) = \xi_\beta \frac{\partial}{\partial \xi_\beta} \bar{U}(\xi_1, \xi_2) - \bar{U}(\xi_1, \xi_2) \quad \text{on} \quad \Delta \ . \tag{2.13}$$

Conditions (2.8), (2.9), together with the anticipated unboundedness of $|\bar{\nabla}\bar{u}|$ as $\bar{r} \to \infty$, suggest that Δ is the upper half-plane $\xi_2 > 0$, with $\underset{\sim}{\xi} \to \underset{\sim}{0}$ as $\bar{r} \to 0$ and vice-versa. Also, if (ρ, φ) are polar coordinates in the closure of this half-plane, so that

$$\xi_1 = \rho \cos\varphi \ , \ \xi_2 = \rho \sin\varphi \quad (0 \le \rho < \infty, \ 0 \le \varphi \le \pi) \ , \tag{2.14}$$

one draws from (2.10) that

$$\rho = \sqrt{\xi_\alpha \xi_\alpha} = |\overline{\nabla u}| \quad . \tag{2.15}$$

Under the transformations (2.10), (2.11) the nonlinear boundary-value problem for $\overline{u}$ on $\mathfrak{F}$ becomes a linear one for $\overline{U}$ on Δ, which — as shown in [2] — admits the explicit solution

$$\overline{U}(\xi_1, \xi_2) = \rho P(\rho) \cos\varphi \quad (0<\rho<\infty,\ 0\le\varphi\le\pi) \ , \tag{2.16}$$

where

$$P(\rho) = \frac{\mu}{2}\int_\rho^\infty \frac{dt}{t^3 W'(3+t^2)} = \mu \int_\rho^\infty \frac{dt}{t^2 \tau(t)} \quad (0<\rho<\infty) \ . \tag{2.17}$$[1]

On setting

$$Q(\rho) = -\rho P'(\rho) \quad (0<\rho<\infty) \ , \tag{2.18}$$

one infers from (2.16), (2.12), in view of (2.3), (2.6), and (2.14), that

$$\left.\begin{aligned} \overline{x}_1 &= \overline{r}\cos\theta = P(\rho) - Q(\rho)\cos^2\varphi \ , \\ \overline{x}_2 &= \overline{r}\sin\theta = -Q(\rho)\sin\varphi\cos\varphi \\ &\qquad (0<\rho<\infty,\ 0\le\varphi\le\pi) \ . \end{aligned}\right\} \tag{2.19}$$

It can be shown[2] that for an <u>elliptic</u> material, equations (2.19) are invertible: for each $\overline{r}>0$ and each θ in the interval $[-\pi, \pi]$ there exist unique values $\rho = \rho(\overline{r}, \overline{\theta})$ and $\varphi = \varphi(\overline{r}, \theta)$, with $\rho > 0$ and φ in $[0, \pi]$,

---

[1] The convergence of the improper integral is assured by the ellipticity condition $\tau' > 0$ on $[0, \infty)$.

[2] A proof of this is sketched in [2] merely for the limiting elliptic power-law material.

such that (2.19) hold. Once $\rho(\bar{r}, \theta)$ and $\varphi(\bar{r}, \theta)$ are known, the desired solution for $\bar{u}(\bar{x}_1, \bar{x}_2)$ in the physical domain follows from (2.13) with the aid of (2.14), (2.16), and (2.3). In this manner, bearing (2.18) in mind, one arrives at

$$\bar{u}(\bar{x}_1, \bar{x}_2) = -\rho Q(\rho) \cos\varphi \quad (0<\bar{r}<\infty, \ -\pi \le \theta < \pi) \ . \tag{2.20}$$

Further, one can verify a posteriori that this algorithm indeed produces a solution of the boundary-value problem (2.7), (2.8), (2.9) with the requisite regularity properties. In the elliptic case considered so far, $\bar{u}$ so determined has continuous partial derivatives of all orders on the entire open region $\mathfrak{D}$. The stresses associated with $\bar{u}$ are obtainable from (1.22), (1.23).

3. Elliptic and hyperbolic solutions of the displacement equation of equilibrium for the special material.

Wtih a view toward exploring the effect of a breakdown of ellipticity on the solution to the small-scale nonlinear crack problem, we turn now to the special "pilot material" introduced in (1.31), whose response to a simple shear is governed by (1.32). When the ellipticity of the required solution field is not guaranteed in advance, the hodograph mapping (2.10) may not be one-to-one and (2.19) need no longer be uniquely invertible. As will be shown, however, even in these circumstances (2.16) to (2.20) may be used to generate solutions of the partial differential equation (2.7) on certain subdomains of $\mathfrak{D}$. These solutions, in turn, may be combined to construct a solution of restricted smoothness to the global boundary-value problem at hand.

The particular choice of the pilot material determined by the

simple-shear response (1.32) was motivated in part by the fact that the integral in (2.17) may be evaluated explicitly for this special incompressible elastic solid. Indeed, (1.32), (2.17), (2.18) give

$$\left.\begin{aligned} &P(\rho) = \frac{1}{2\rho^2} + \frac{3}{2} \quad (0<\rho\le 1)\ , \quad P(\rho) = \frac{2}{\sqrt{\rho}} \quad (1\le\rho<\infty)\ , \\ &Q(\rho) = \frac{1}{\rho^2} \quad (0<\rho\le 1)\ , \quad Q(\rho) = \frac{1}{\sqrt{\rho}} \quad (1\le\rho<\infty)\ . \end{aligned}\right\} \tag{3.1}$$

Equations (2.19) may be rewritten as

$$\left.\begin{aligned} &\bar{x}_1 = \bar{r}\cos\theta = a(\rho) - b(\rho)\cos 2\varphi\ , \\ &\bar{x}_2 = \bar{r}\sin\theta = -b(\rho)\sin 2\varphi \quad (0<\rho<\infty,\ 0\le\varphi\le\pi) \end{aligned}\right\} \tag{3.2}$$

with

$$a(\rho) = P(\rho) - \tfrac{1}{2}Q(\rho)\ , \quad b(\rho) = \tfrac{1}{2}Q(\rho)\ . \tag{3.3}$$

Thus, regardless of the <u>specific</u> choice of the material, the points $(\bar{x}_1, \bar{x}_2)$ in the physical plane that correspond to a constant positive value of ρ comprise the circle

$$\Gamma(\rho) : [\bar{x}_1 - a(\rho)]^2 + \bar{x}_2^2 = b^2(\rho)\ , \tag{3.4}$$

which is centered at $(a(\rho), 0)$ and has $b(\rho)$ as its radius.

Returning to the pilot material and <u>confining our attention to</u> $0<\rho<1$ for the time being, we note that (3.1) to (3.4) yield $a(\rho) = 3/2$, $b(\rho) = 1/2\rho^2$ and

$$\left.\begin{aligned} &\bar{x}_1 - \frac{3}{2} = -\frac{1}{2\rho^2}\cos 2\varphi\ ,\quad x_2 = -\frac{1}{2\rho^2}\sin 2\varphi\quad (0<\rho<1,\ 0\le\varphi\le\pi)\ , \\ &\Gamma(\rho):\ (\bar{x}_1 - \tfrac{3}{2})^2 + \bar{x}_2^2 = \frac{1}{4\rho^4}\quad (0<\rho<1)\ . \end{aligned}\right\} \tag{3.5}$$

Consequently, if $(\bar{r}_1, \theta_1)$ are polar coordinates at $\bar{x}_1 = 3/2$, $\bar{x}_2 = 0$ (see Figure 5(a)), so that

$$\left.\begin{aligned} &\bar{x}_1 = \bar{r}\cos\theta = \frac{3}{2} + \bar{r}_1\cos\theta_1\ , \\ &\bar{x}_2 = \bar{r}\sin\theta = \bar{r}_1\sin\theta_1\quad (0\le\bar{r}_1<\infty,\ -\pi\le\theta_1<\pi)\ , \end{aligned}\right\} \tag{3.6}$$

one has from (3.5),

$$\rho = (2\bar{r}_1)^{-1/2}\ ,\quad \varphi = \frac{1}{2}(\theta_1 + \pi)\ . \tag{3.7}$$

Further, (3.1), (3.7), (2.20) and $0<\rho<1$ now give

$$\bar{u} = e(\bar{x}_1, \bar{x}_2) = (2\bar{r}_1)^{1/2}\sin\frac{\theta_1}{2}\ \text{ on }\ \mathcal{E}\ , \tag{3.8}$$

where $\mathcal{E}$ is the subdomain of $\mathfrak{D}$ defined by

$$\mathcal{E} = \{(\bar{r}, \theta)\,|\,\tfrac{1}{2}<\bar{r}_1<\infty,\ -\pi<\theta_1<\pi\} \tag{3.9}$$

and indicated in Figure 5(a). As $\rho\to 1$ in the last of (3.5), $\Gamma(\rho)$ tends to the circle

$$\mathcal{C}:\ (\bar{x}_1 - \tfrac{3}{2})^2 + \bar{x}_2^2 = \tfrac{1}{4}\ \text{ or }\ \bar{r}_1 = \tfrac{1}{2}\ ,\ -\pi\le\theta_1<\pi\ . \tag{3.10}$$

The boundary of $\mathcal{E}$ thus consists of $\mathcal{C}$ and the half-line $-\infty<\bar{x}_1<1$, $\bar{x}_2 = 0$.

Since the partial differential equation (2.7) reduces to Laplace's

equation for the pilot material in case $\rho<1$, the displacement (3.8) evidently satisfies the appropriate specialized version of (2.7) on $\mathcal{E}$. Moreover, from (3.8), (3.9) follows

$$|\overline{\nabla}\overline{u}| = |\overline{\nabla}e| = \rho = (2\overline{r}_1)^{-1/2} < 1 \quad \text{on} \quad \mathcal{E} \ , \tag{3.11}$$

whence the solution (3.8) is elliptic throughout the open region $\mathcal{E}$. Clearly, $|\overline{\nabla}e| \to 1$ as a point on C is approached. It is essential to observe that the elliptic solution e is discontinuous across the half-axis $-\infty<\overline{x}_1<1$, $\overline{x}_2=0$, rather than merely across the semi-infinite crack $-\infty<\overline{x}_1<0$, $\overline{x}_2=0$. In fact, as is apparent from (2.6), (2.1) and the remarks following (2.1), the solution under discussion coincides with the near field of the out-of-plane displacement for a Neo-Hookean material and a crack tip situated at $\overline{r}_1=0$, rather than at the origin $r=0$.

We proceed now to the case $\rho>1$. In this instance (3.1) to (3.4) furnish $a(\rho)=3/2\sqrt{\rho}$, $b(\rho)=1/2\sqrt{\rho}$

$$\left.\begin{aligned} &\overline{x}_1=\overline{r}\cos\theta=\frac{1}{2\sqrt{\rho}}(3-\cos 2\varphi) \ , \\ &\overline{x}_2=\overline{r}\sin\theta=-\frac{1}{2\sqrt{\rho}}\sin 2\varphi \quad (1<\rho<\infty,\ 0\le\varphi\le\pi) \ , \\ &\Gamma(\rho):\left(\overline{x}_1-\frac{3}{2\sqrt{\rho}}\right)^2+\overline{x}_2^2=\frac{1}{4\rho} \quad (1<\rho<\infty) \ . \end{aligned}\right\} \tag{3.12}$$

Upon referring the last of (3.12) to the polar coordinates $(\overline{r},\theta)$ and solving the resulting quadratic equation in $\sqrt{\rho}$, one is led to

$$\sqrt{\rho}=\frac{1}{2\overline{r}}[3\cos\theta\pm R(\theta)] \ , \tag{3.13}$$

provided

$$R(\theta) = \sqrt{9\cos^2\theta - 8} \quad . \tag{3.14}$$

On the other hand, (3.13), (3.14) and the first two of (3.12), after some algebraic manipulations, are found to imply

$$\left.\begin{aligned} \cos\varphi &= \frac{-2\sqrt{2}\sin\theta}{[1+3\sin^2\theta \pm R(\theta)\cos\theta]^{1/2}} \quad , \\ \sin\varphi &= \frac{\cos\theta \pm R(\theta)}{\sqrt{2}[1+3\sin^2\theta \pm R(\theta)\cos\theta]^{1/2}} \quad . \end{aligned}\right\} \tag{3.15}$$

Clearly, both values of $\sqrt{\rho}$ supplied by (3.13) are real and positive if and only if

$$|\cos\theta| \le \sqrt{8/9} \quad \text{or} \quad -\theta_0 \le \theta \le \theta_0 \ , \ \theta_0 = \cos^{-1}(\sqrt{8}/3) \quad . \tag{3.16}$$

Further, since $\rho > 1$ at present, (3.13) demands that

$$3\cos\theta \pm R(\theta) > 2\overline{r} \quad . \tag{3.17}$$

Now let $\mathfrak{N}^+$ and $\mathfrak{N}^-$ be the two subdomains of $\mathfrak{D}$ defined by

$$\left.\begin{aligned} \mathfrak{N}^+ &= \{(\overline{r},\theta) \,|\, 0 < \overline{r} < \tfrac{1}{2}[3\cos\theta + R(\theta)] \ , \ 0 \le |\theta| < \theta_0\} \quad , \\ \mathfrak{N}^- &= \{(\overline{r},\theta) \,|\, 0 < \overline{r} < \tfrac{1}{2}[3\cos\theta - R(\theta)] \ , \ 0 < |\theta| < \theta_0\} \quad , \end{aligned}\right\} \tag{3.18}$$[1]

which are shown in Figure 5(b) and Figure 5(c), respectively, and which evidently conform to (3.16), as well as to the inequality (3.17) with the

---

[1] The reason for excluding points on the ray $\theta = 0$ from $\mathfrak{N}^-$ will emerge presently.

appropriate sign alternative.

For the purpose of examining the geometry of the two open point sets $\overset{+}{\mathcal{N}}$ and $\overset{-}{\mathcal{N}}$ we note first that $\Gamma(\rho)$ in the last of (3.12), as $\rho \to 1$, tends to circle C given by (3.10). Next, let $\overset{+}{C}$ and $\overset{-}{C}$ be the two complementary circular arcs of C defined by

$$\left.\begin{aligned} \overset{+}{C} &= \{(\overline{r}_1, \theta_1) \,|\, \overline{r}_1 = \tfrac{1}{2}\,,\ 0 \le |\theta_1| \le \theta_0 + \tfrac{\pi}{2}\}\,, \\ \overset{-}{C} &= \{(\overline{r}_1, \theta_1) \,|\, \overline{r}_1 = \tfrac{1}{2}\,,\ \theta_0 + \tfrac{\pi}{2} < |\theta_1| \le \pi\}\,, \end{aligned}\right\} \quad (3.19)$$

and observe on the basis of (3.6), (3.14), (3.16) that these two arcs may also be described by

$$\left.\begin{aligned} \overset{+}{C} &= \{(\overline{r}, \theta) \,|\, \overline{r} = \tfrac{1}{2}[3\cos\theta + R(\theta)]\,,\ 0 \le |\theta| \le \theta_0\}\,, \\ \overset{-}{C} &= \{(\overline{r}, \theta) \,|\, \overline{r} = \tfrac{1}{2}[3\cos\theta - R(\theta)]\,,\ 0 \le |\theta| < \theta_0\}\,. \end{aligned}\right\} \quad (3.20)$$

It is clear from (3.18), (3.20) that the boundary of $\overset{+}{\mathcal{N}}$ consists of the two ray-segments $0 \le \overline{r} \le \sqrt{2}$, $\theta = \pm\theta_0$ together with the circular arc $\overset{+}{C}$, as indicated in Figure 5(b); in contrast, the boundary of $\overset{-}{\mathcal{N}}$ — displayed in Figure 5(c) — is now seen to be composed of the same two ray-segments, the circular arc $\overset{-}{C}$, as well as the segment $0 \le \overline{r} \le 1$, $\theta = 0$ of the $\overline{x}_1$-axis.

Recalling from (3.1) that $Q(\rho) = 1/2\sqrt{\rho}$ when $\rho > 1$ and substituting from (3.13) and the first of (3.15) into (2.20), we arrive at the two out-of-plane displacement fields:

$$\left.\begin{aligned} \bar{u} = \overset{+}{h}(\bar{x}_1, \bar{x}_2) &= \frac{[3\cos\theta + R(\theta)]^{3/2}\sin\theta}{\sqrt{2}\,\bar{r}[\cos\theta + R(\theta)]^{1/2}} \quad \text{on } \overset{+}{\mathscr{R}} \\ \bar{u} = \bar{h}(\bar{x}_1, \bar{x}_2) &= \frac{[3\cos\theta - R(\theta)]^{3/2}\sin\theta}{\sqrt{2}\,\bar{r}[\cos\theta - R(\theta)]^{1/2}} \quad \text{on } \bar{\mathscr{R}} \end{aligned}\right\} \tag{3.21}$$

with $R(\theta)$ given by (3.14). Both $\overset{+}{h}$ and $\bar{h}$ are real-valued functions that have continuous partial derivatives of all orders on their respective domains of definition; further, each satisfies the displacement-equation of equilibrium (2.7), specialized for the pilot material and $\rho > 1$, as is readily verified by substitution. Also, a direct computation confirms — in agreement with (2.15) and (3.13) — that

$$\left.\begin{aligned} |\bar{\nabla}\bar{u}| = |\bar{\nabla}\overset{+}{h}| &= \frac{1}{4\bar{r}^2}[3\cos\theta + R(\theta)]^2 > 1 \quad \text{on } \overset{+}{\mathscr{R}}\,, \\ |\bar{\nabla}\bar{u}| = |\bar{\nabla}\bar{h}| &= \frac{1}{4\bar{r}^2}[3\cos\theta - R(\theta)]^2 > 1 \quad \text{on } \bar{\mathscr{R}}\,, \end{aligned}\right\} \tag{3.22}$$

so that $\overset{+}{h}$ and $\bar{h}$ are both hyperbolic solutions throughout the open sets $\overset{+}{\mathscr{R}}$ and $\bar{\mathscr{R}}$, respectively. From (3.22) and (3.20) one infers that $|\bar{\nabla}\overset{+}{h}| \to 1$ as a point on the boundary-segment $\overset{+}{C}$ of $\overset{+}{\mathscr{R}}$ is approached; similarly, $|\bar{\nabla}\bar{h}| \to 1$ at every point of the circular arc $\bar{C}$.

Finally, (3.14) and the second of (3.21) reveal that

$$\bar{h}(\bar{x}_1, 0\pm) = \pm\frac{1}{\bar{x}_1} \quad (0 < \bar{x}_1 < 1)\,. \tag{3.23}$$

Consequently, the second of the foregoing two hyperbolic solutions has a finite jump discontinuity across the segment $0 < \bar{x}_1 < 1$ of the $\bar{x}_1$-axis.

4. Construction of a solution to the small-scale nonlinear crack problem for the pilot material.

In this section we attempt to piece together the solutions of the partial differential equation (2.7) established in Section 3 in order to construct a solution – continuous and piecewise smooth on $\mathfrak{D}$ – of the small-scale nonlinear crack problem (2.7), (2.8), (2.9) for the pilot material.

To this end we note first that we have available only the elliptic solution e on the complement of $\mathcal{N}^+$ with respect to the cut plane $\mathfrak{D}$ and only the hyperbolic solution h^+ in the interior of the circle C (see Figure 5). Further, as is easily seen from (3.8), (3.21) and (3.6), (3.14), both e and $\bar{\nabla}e$ join continuously with h^+ and $\bar{\nabla}h^+$ across the circular arc C^+ separating the elliptic domain $\mathcal{E}$ and the hyperbolic domain $\mathcal{N}^+$. Thus e and h^+ supply a solution of the requisite smoothness to the differential equation (2.7) at all points of $\mathfrak{D}$ that lie outside the boundary of $\bar{\mathcal{N}}$.

Since h^+ is the only one of the three solutions available on $\bar{\mathcal{N}}$ that is continuous across the segment $0<\bar{x}_1<1$ of the $\bar{x}_1$-axis, it follows that the solution to the boundary-value problem (2.7), (2.8), (2.9) we are trying to assemble must coincide with h^+ in the vicinity of this segment. On the other hand, the transition from h^+ to e across the ray-segments $0\le\bar{r}\le\sqrt{2}$, $\theta=\pm\theta_0$ is readily found to involve a jump discontinuity in $\bar{u}$.

The foregoing considerations suggest that we dismiss $\bar{h}$ altogether and seek to "match" h^+ and e across two as yet undetermined curves $\mathcal{L}$ and $\mathcal{L}'$ (Figure 6) that are symmetrically situated with respect to the $\bar{x}_1$-axis, start at the origin, terminate at the points $\bar{r}=\sqrt{2}$, $\theta=\pm\theta_0$, and otherwise lie wholly in $\bar{\mathcal{N}}$. This matching, moreover, must assure the

continuity of $\bar{u}$ and of the traction across the two curves to be found. As will emerge shortly, there exist unique "shocks" (shock-lines) $\mathscr{S}$ and $\mathscr{S}'$ with the desired properties; as either of these lines is traversed $\bar{u}$ and its tangential derivative remain continuous, while the normal derivative of $\bar{u}$ suffers a finite jump discontinuity — despite the prevailing traction continuity across $\mathscr{S}$ and $\mathscr{S}'$.

The final solution of the small-scale yielding problem thus obtained coincides with the hyperbolic solution $\overset{+}{h}$ on the finite domain $\mathscr{R}_*$ whose boundary is the closed curve composed of $\mathscr{S}$, $\mathscr{S}'$, and $\overset{+}{C}$ (see Figure 6); it coincides with the elliptic solution e on the domain $\mathscr{E}_*$ consisting of all points of $\mathscr{D}$ exterior to the boundary of $\mathscr{R}_*$. Since $\bar{r}_1 \sim \bar{r}$ and $\theta_1 \sim \theta$ as $\bar{r} \to \infty$, it is clear from (3.8) that the composite solution just described satisfies the conditions (2.9) at infinity, in addition to the boundary conditions (2.8), which are obviously met. While the solution here alluded to clearly possesses the required (relaxed) smoothness on $\mathscr{D}$, we shall have to show eventually that $\bar{u}$ so determined remains bounded as $\bar{r} \to 0$.

We proceed now to the determination of the upper shock $\mathscr{S}$, from which $\mathscr{S}'$ follows by symmetry. Since the hyperbolic solution $\bar{h}$ has been discarded, we shall henceforth write h in place of $\overset{+}{h}$. According to (3.8) and (3.21), the two solutions of (2.7) to be matched across the desired curve $\mathscr{S}$ are:

$$\left.\begin{aligned} \bar{u} &= e(\bar{x}_1, \bar{x}_2) = (2\bar{r}_1)^{1/2} \sin\frac{\theta_1}{2} \quad \text{on } \mathscr{E}\,, \\ \bar{u} &= h(\bar{x}_1, \bar{x}_2) = \frac{f(\theta)}{\bar{r}} \quad \text{on } \overset{+}{\mathscr{R}}\,, \end{aligned}\right\} \tag{4.1}$$

where

$$f(\theta) = \frac{1}{\sqrt{2}} \frac{[3\cos\theta + R(\theta)]^{3/2} \sin\theta}{[\cos\theta + R(\theta)]^{1/2}} \quad , \quad R(\theta) = \sqrt{9\cos^2\theta - 8} \quad . \tag{4.2}$$

The continuity of the displacement $\bar{u}$ across $\mathscr{S}$ therefore demands that

$$(2\bar{r}_1)^{1/2} \sin\frac{\theta_1}{2} = \frac{f(\theta)}{\bar{r}} \quad \text{on } \mathscr{S} \ , \tag{4.3}$$

in which $\bar{r}_1$ and θ_1, on account of (3.6), may be regarded as functions of $\bar{r}$ and θ. We shall show that (4.3) actually admits a unique solution

$$\mathscr{S} : \bar{r} = \hat{r}(\theta) \quad (0 \le \theta \le \theta_0) \ , \ \hat{r}(0) = 0, \hat{r}(\theta_0) = \sqrt{2} \tag{4.4}$$

and that the emerging shock $\mathscr{S}$ meets all the conditions stated earlier.

With a view toward proving this claim, we temporarily take for granted the existence of a solution (4.4) to (4.3) and infer, with the aid of (3.6), that then necessarily

$$\hat{r}^6 \sin^2\theta - 2\hat{r}^3 f^2(\theta)\cos\theta + 3\hat{r}^2 f^2(\theta) - f^4(\theta) = 0 \quad . \tag{4.5}$$

Next, we introduce the auxiliary function

$$\zeta = \zeta(\theta) = \frac{\hat{r}(\theta)}{3\cos\theta + R(\theta)} \quad (0 \le \theta \le \theta_0) \tag{4.6}$$

and use (4.2) to conclude, after lengthy elementary manipulations, that (4.5) may now be written as

$$(\zeta - \tfrac{1}{2})^2 \left\{ \zeta^4 + \zeta^3 + \frac{3}{4}\zeta^2 - (4\zeta + 1)\frac{\sin^2\theta}{[\cos\theta + R(\theta)]^2} \right\} = 0 \quad . \tag{4.7}$$

But (4.6) and (3.20) imply that the first factor in (4.7) vanishes if and only

if $\bar{r} = \hat{r}(\theta)$ and θ are the polar coordinates of a point on the circular arc $\overset{+}{C}$ and hence this factor cannot vanish on $\mathscr{S}$. The presence of the root $\zeta = 1/2$ of (4.7) merely reflects the continuity of $\bar{u}$ across $\overset{+}{C}$ mentioned previously. It follows that the function within braces in (4.7) must vanish on $\mathscr{S}$, so that

$$\left.\begin{aligned} \phi(\zeta) \equiv \frac{\zeta^4 + \zeta^3 + \frac{3}{4}\zeta^2}{4\zeta + 1} = \frac{\sin^2\theta}{[\cos\theta + R(\theta)]^2} \equiv \psi(\theta) \\ (0 \le \theta \le \theta_0) \quad \text{on } \mathscr{S} \ . \end{aligned}\right\} \quad (4.8)$$

The function ψ appearing in (4.8) is strictly increasing on $[0, \theta_0]$, with $\psi(0) = 0$ and $\psi(\theta_0) = 1/8$, whereas the rational function ϕ on the left side of this equation is easily seen to increase steadily from $\phi(0) = 0$ to $\phi(1/2) = 1/8$ as ζ ranges over the interval $[0, 1/2]$. Consequently, for each given θ in $[0, \theta_0]$ there exists precisely one root $\zeta = \zeta(\theta)$ of (4.8). If we now employ (4.6) to <u>define</u> $\hat{r}(\theta)$ and reverse the steps that led from (4.3) to (4.8), <u>we infer the existence and uniqueness of the shock</u> $\mathscr{S}$ described by (4.4).

Although (4.8) has not been solved explicitly for $\zeta = \zeta(\theta)$, the numerical calculation of $\hat{r}(\theta)$ $(0 \le \theta \le \theta_0)$ from (4.8), (4.6) presents no difficulties. The results of this computation are plotted in Figure 6. Further, equations (4.8), (4.6) enable one to extract the asymptotic behavior of the shock $\mathscr{S}$ near its endpoints. One finds in this manner that

$$\left.\begin{aligned} \hat{r}(\theta) &\sim \frac{4}{\sqrt{3}}\sin\theta \quad \text{as} \quad \theta \to 0 \ , \\ \hat{r}(\theta) &\sim \sqrt{2} - 2^{5/4}(\theta_0 - \theta)^{1/2} \quad \text{as} \quad \theta \to \theta_0 \ . \end{aligned}\right\} \quad (4.9)$$

As is easily verified, (4.9) assures that $\mathscr{S}$ is tangential to the $\bar{x}_1$-axis at the origin and tangential to the circle $\mathcal{C}$ at $\bar{r} = \sqrt{2}$, $\theta = \theta_0$.

Our next objective is to establish the continuity of the tractions across the shock $\mathscr{S}$. In this connection we rely on (1.24), (1.19), and (2.6) to see that the only non-vanishing nominal traction component along $\mathscr{S}$ is given by

$$s \equiv s_3 = 2W'(3 + |\bar{\nabla}\bar{u}|^2)\frac{\partial \bar{u}}{\partial n} , \tag{4.10}$$

where $\bar{u} = e$ on the elliptic side of $\mathscr{S}$, while $\bar{u} = h$ on the hyperbolic side. Denoting the scalar traction s on the two sides of $\mathscr{S}$ by s_e and s_h, respectively, we draw from (4.10) and (1.26), (1.32) that

$$s_e = \mu \frac{\partial e}{\partial n} , \quad s_h = \mu |\bar{\nabla} h|^{-3/2} \frac{\partial h}{\partial n} . \tag{4.11}$$

Accordingly, the tractions are continuous across $\mathscr{S}$ if and only if

$$s_h - s_e = 0 \quad \text{or} \quad \left\{ |\bar{\nabla} h|^{-3/2} \bar{\nabla} h - \bar{\nabla} e \right\} \cdot \underset{\sim}{n} = 0 \quad \text{on } \mathscr{S} , \tag{4.12}$$

provided $\underset{\sim}{n}$ is a unit normal vector of $\mathscr{S}$ and the dot signifies scalar multiplication. Keeping in mind that the displacement-continuity condition (4.3), which determined the shock $\mathscr{S}$, asserts

$$h - e = 0 \quad \text{on } \mathscr{S} , \tag{4.13}$$

one has

$$\underset{\sim}{n} = \frac{\bar{\nabla} h - \bar{\nabla} e}{|\bar{\nabla} h - \bar{\nabla} e|} \quad \text{on } \mathscr{S} . \tag{4.14}$$

The traction-continuity condition (4.12) is therefore equivalent to

$$|\bar{\nabla}h|^{1/2}+|\bar{\nabla}e|^{2}-\left\{1+|\bar{\nabla}h|^{-3/2}\right\}\bar{\nabla}h\cdot\bar{\nabla}e=0 \quad \text{on } \mathscr{S} \, . \tag{4.15}$$

Aiming at a verification of (4.15), we first record the polar components of $\bar{\nabla}h$, which follow from the second of (4.1):

$$\frac{\partial h}{\partial \bar{r}}=-\frac{1}{\bar{r}^{2}}f(\theta) \, , \quad \frac{1}{\bar{r}}\frac{\partial h}{\partial \theta}=\frac{1}{\bar{r}^{2}}\dot{f}(\theta) \, . \tag{4.16}$$[1]

Similarly, the first of (4.1), in conjunction with (3.6), enables one to arrive at

$$\frac{\partial e}{\partial \bar{r}}=\frac{1}{\sqrt{2\bar{r}_{1}}}\sin\left(\theta-\frac{\theta_{1}}{2}\right) \, , \quad \frac{1}{\bar{r}}\frac{\partial e}{\partial \theta}=\frac{1}{\sqrt{2\bar{r}_{1}}}\cos\left(\theta-\frac{\theta_{1}}{2}\right) \, . \tag{4.17}$$

Equations (4.16), (4.17) reduce (4.15) to

$$\frac{1}{2\bar{r}_{1}}+\frac{1}{\bar{r}}\left[f^{2}(\theta)+\dot{f}^{2}(\theta)\right]^{1/4}$$

$$-\frac{1}{\bar{r}^{2}\sqrt{2\bar{r}_{1}}}\left\{1+\bar{r}^{3}\left[f^{2}(\theta)+\dot{f}^{2}(\theta)\right]^{-3/4}\right\}F(\theta)=0 \quad \text{on } \mathscr{S} \, , \tag{4.18}$$

with

$$F(\theta)=\dot{f}(\theta)\cos\left(\theta-\frac{\theta_{1}}{2}\right)-f(\theta)\sin\left(\theta-\frac{\theta_{1}}{2}\right) \, . \tag{4.19}$$

Now, (3.6) and (4.3) justify

$$\bar{r}=\left[\frac{f^{2}(\theta)\sin\theta_{1}}{2\sin\theta\sin^{2}(\theta_{1}/2)}\right]^{1/3} \, , \quad \bar{r}_{1}=\left[\frac{f(\theta)\sin\theta}{\sqrt{2}\sin(\theta_{1}/2)\sin\theta_{1}}\right]^{2/3} \quad \text{on } \mathscr{S} \, . \tag{4.20}$$

---

[1] Here and in what follows $\dot{f}$ stands for the derivative of f.

Finally, substitution from (4.20) into (4.18) and subsequent use of the definition (4.2) of $f(\theta)$, after a lengthy computation, confirm that (4.18) is indeed satisfied. This completes the verification of the traction-continuity requirement (4.12).

We have yet to show that the solution $\bar{u}$ constructed in this section remains bounded as $\bar{r} \to 0$. According to the first of (4.1), the restriction of e to the final elliptic domain $\mathcal{E}_*$ (Figure 6) clearly meets this condition. It therefore suffices to prove that the hyperbolic solution h is bounded on the point-set $\mathcal{P}$ consisting of all points $(\bar{r}, \theta)$ with $\bar{r} > 0$, $\theta \geq 0$ that belong either to $\mathcal{H}_*$ or to $\mathcal{I}$. Note that $\mathcal{P}$ is the closure of the upper half of the final hyperbolic domain $\mathcal{H}_*$, with the exception of the origin.

Since $\mathcal{I}$ is tangential to the $\bar{x}_1$-axis at the origin[1], it follows that every ray from this point to a point in $\mathcal{P}$ intersects $\mathcal{I}$ precisely once, whence

$$\bar{r} \geq \hat{r}(\theta) \quad \text{for all } (\bar{r}, \theta) \text{ in } \mathcal{P} \ . \tag{4.21}$$

We recall next that $\zeta(\theta)$ in (4.8) has the range $[0, 1/2]$, so that

$$\zeta(\theta) \geq \sqrt{\frac{2}{3}} \frac{\sin\theta}{\cos\theta + R(\theta)} \quad (0 \leq \theta \leq \theta_0) \tag{4.22}$$

and (4.6) yields the lower bound

$$\hat{r}(\theta) \geq \sqrt{\frac{2}{3}} \frac{[3\cos\theta + R(\theta)]}{[\cos\theta + R(\theta)]} \sin\theta \quad (0 \leq \theta \leq \theta_0) \tag{4.23}$$

But (4.21) and the second of (4.1) give

---

[1] Refer to the first of (4.9).

$$h(\bar{x}_1, \bar{x}_2) = \frac{f(\theta)}{\bar{r}} \leq \frac{f(\theta)}{\hat{r}(\theta)} \quad \text{on } \mathscr{C} , \tag{4.24}$$

while this inequality, together with (4.23) and (4.2), leads to

$$h(\bar{x}_1, \bar{x}_2) \leq \frac{\sqrt{3}}{2}\{[3\cos\theta + R(\theta)][\cos\theta + R(\theta)]\}^{1/2} \leq \sqrt{6} \quad \text{on } \mathscr{C} . \tag{4.25}$$

This establishes the required boundedness of h, and thus of $\bar{u}$, as $\bar{r} \to 0$.

In contrast, $\bar{\nabla}\bar{u}$ fails to remain bounded as the origin is approached from within $\mathscr{R}_*$, as is apparent from the first of (3.22), which gives

$$|\bar{\nabla}\bar{u}(\bar{x}_1, 0)| \sim \frac{4}{\bar{x}_1^2} \quad \text{as } \bar{x}_1 \to 0+ . \tag{4.26}$$

One shows easily that $|\bar{\nabla}\bar{u}| \to \infty$ as $\bar{r} \to 0$ along <u>any</u> regular arc lying in $\mathscr{R}_*$ or along $\mathscr{A}$. In addition, it should be pointed out that (4.1) furnishes

$$\bar{u}(\bar{x}_1, 0\pm) = \pm\sqrt{2\bar{r}_1} \quad (-\infty < \bar{x}_1 < 0) , \quad \bar{u}(\bar{x}_1, 0) = 0 \quad (0 < \bar{x}_1 < \infty) , \tag{4.27}$$

which reveal a displacement discontinuity at the origin.

There is one further requirement that has been proposed for elastostatic fields with discontinuous deformation gradients which has not been mentioned so far in the present paper. This condition insures the dissipative character of the shocks inherent in such a field and is an analogue of the entropy inequality for gas-dynamical shocks.

The elastostatic inequality to which we are alluding was first deduced in [5] with limitation to rectilinear shocks in piecewise homogeneous plane deformations; it was later extended to curved shocks and general non-homogeneous deformations in [6], where the special form assumed by this condition in the particular case of anti-plane shear was given separate

attention[1]. A thermodynamic argument in support of the dissipation condition for compressible elastic materials is produced at the end of [6].

The application to the solution field under consideration of the dissipation inequality referred to above is contingent upon a quasi-static interpretation of this field, in which the amount of shear k applied at infinity plays the role of "time" – or, more appropriately, of a history parameter[2]. In this connection the corresponding velocity $\underset{\sim}{V}(\underset{\sim}{x}, k)$ of a point $\underset{\sim}{x}$ on the instantaneous shock $\mathscr{S}(k)$ relative to the undeformed configuration is of importance[3].

In view of (4.4) and (2.6), the physical position vector of a point on $\mathscr{S}(k)$ is given by

$$\underset{\sim}{x} = \hat{\underset{\sim}{x}}(\theta, k) = ck^2 \hat{r}(\theta)\underset{\sim}{a}(\theta) \quad (0 \le \theta \le \theta_0) \ , \tag{4.28}$$

if $\underset{\sim}{a}(\theta)$ is the radial unit base vector associated with the polar coordinates (r, θ). Hence

$$\underset{\sim}{V}(\underset{\sim}{x}, k) \equiv \frac{\partial}{\partial k}\hat{\underset{\sim}{x}}(\theta, k) = \frac{2}{k}\hat{\underset{\sim}{x}}(\theta, k) \quad (0 \le \theta \le \theta_0) \ . \tag{4.29}$$

It follows from (4.28), (4.29) and properties of the function $\hat{r}$ established earlier that $\underset{\sim}{V}(\underset{\sim}{x}, k)$ always points into the hyperbolic domain $\mathscr{H}_*$, so that – as k increases – material points of the body traverse the shock $\mathscr{S}(k)$ from the hyperbolic "upstream" to the elliptic "downstream" side of $\mathscr{S}(k)$. The

---

[1] See Section 6 of [6].

[2] Thus as "time" k increases, the body undergoes loading, rather than unloading.

[3] By virtue of the symmetry of the solution $\bar{u}$ at hand we may confine the following considerations to the upper shock.

relevant dissipation inequality[1] now takes the form of the jump condition

$$[H]^+_- \leq 0 \quad \text{on } \mathscr{S} , \tag{4.30}$$

in which the function within brackets is defined by

$$H = -W(3 + |\nabla u|^2) + 2W'(3 + |\nabla u|^2)\left(\frac{\partial u}{\partial n}\right)^2 \tag{4.31}$$[2]

and $[H]^+_-$ stands for the difference between the limiting value of H on the upstream (or positive) side of $\mathscr{S}$ and its limiting value on the downstream (or negative) side. On account of (4.31), (4.10), (2.6), and the continuity of the tractions across $\mathscr{S}$, we arrive at

$$[H]^+_- = -[W]^+_- + s\left[\frac{\partial \bar{u}}{\partial n}\right]^+_- \quad \text{on } \mathscr{S} , \; W = W(3 + |\bar{\nabla}\bar{u}|^2) . \tag{4.32}$$

Recalling that $\bar{u} = h$ on the upstream side, while $\bar{u} = e$ on the downstream side of $\mathscr{S}$, we now express the right-hand member in the first of (4.32) in terms of $\bar{\nabla}h$ and $\bar{\nabla}e$. To this end we first invoke (1.31), (1.19), and (2.6), which give

$$[W]^+_- = \frac{\mu}{2}\{4|\bar{\nabla}h|^{1/2} - 3 - |\bar{\nabla}e|^2\} , \tag{4.33}$$

whereas (4.11) and the first of (4.12) enable us to write

$$s\left[\frac{\partial \bar{u}}{\partial n}\right]^+_- = \mu |\bar{\nabla}h|^{-3/2} \bar{\nabla}h \cdot \underset{\sim}{n}(\bar{\nabla}h \cdot \underset{\sim}{n} - \bar{\nabla}e \cdot \underset{\sim}{n}) . \tag{4.34}$$

Furthermore, another appeal to (4.11), (4.12) yields

---

[1] See (4.19) and (6.13) in [6].

[2] Here $\partial u/\partial n = \nabla u \cdot \underset{\sim}{n}$ and $\underset{\sim}{n}$ is a unit normal vector of $\mathscr{S}$.

$$\overline{\nabla}e\cdot\underset{\sim}{n} = |\overline{\nabla}h|^{-3/2}\overline{\nabla}h\cdot\underset{\sim}{n} \ . \tag{4.35}$$

Using this result in (4.34) and thereafter substituting from (4.33), (4.34) into (4.32), we are finally led to

$$[H]^{+}_{-} = \frac{\mu}{2}\left\{ |\overline{\nabla}e|^2 + 3 - 4|\overline{\nabla}h|^{1/2} + \frac{2(\overline{\nabla}h\cdot\underset{\sim}{n})^2}{|\overline{\nabla}h|^{3/2}}\left[1 - |\overline{\nabla}h|^{-3/2}\right]\right\} \ . \tag{4.36}$$

We turn next to a verification of the dissipation inequality (4.30) at the endpoints of the shock $\mathscr{S}$. Since $|\overline{\nabla}h|>1$, (4.36) implies that

$$[H]^{+}_{-} \le \frac{\mu}{2}\{ |\overline{\nabla}e|^2 - 2|\overline{\nabla}h|^{1/2} + 3\} \quad \text{on } \mathscr{S} \ . \tag{4.37}$$

But according to (3.11) and (3.22), $|\overline{\nabla}e|$ is bounded and $|\overline{\nabla}h|\to\infty$ as $\overline{r}\to 0$. Consequently, (4.30) is certain to hold along $\mathscr{S}$ in a neighborhood of the origin.

The confirmation of (4.30) near the right endpoint of $\mathscr{S}$, at $\overline{r}=\sqrt{2}$, $\theta=\theta_0$, unfortunately turns out to be a very cumbersome task, which requires a considerable improvement of the second estimate in (4.9). The requisite refinement of this asymptotic result is found to be

$$\hat{f}(\theta) = \sqrt{2} - 2^{5/4}(\theta_0-\theta)^{1/2} + \frac{5}{4}(\theta_0-\theta) - 226\times 2^{-13/4}(\theta_0-\theta)^{3/2} + O\{(\theta_0-\theta)^2\} \ \text{ as } \theta\to\theta_0 \ , \tag{4.38}$$

and calculations far too elaborate to be included here eventually yield

$$[H]^{+}_{-} = -33\times 2^{1/4}(\theta_0-\theta)^{3/2} + O\{(\theta_0-\theta)^2\} \ \text{ as } \theta\to\theta_0 \ . \tag{4.39}$$

It is now evident that (4.30) also holds in a neighborhood of the right endpoint of $\mathscr{S}$. Numerical calculations, which were carried out on the basis of (4.36), reveal that the dissipation inequality is in fact satisfied at all points of the shock.

In defining the pilot material through (1.31) we assumed for convenience that the peak of the response curve in simple shear (Figure 3) is situated at $k = 1$. If this normalization is abandoned and the maximum of $\tau(k)$ is permitted to occur instead at $k = k_0$ $(k_0 > 0)$, (1.32) give way to

$$\tau(k) = \mu k \quad (0 \leq k \leq k_0) \ , \ \tau(k) = \mu k_0 (k/k_0)^{-1/2} \quad (k_0 \leq k < \infty) \ , \tag{4.40}$$

while (1.31) undergo an analogous modification in accordance with (1.27). It is easily seen that in these circumstances the physical problem governed by (1.18), (2.4), (2.5) again reduces to the dimensionless version (2.7), (2.8), (2.9) provided the scaling (2.6) is replaced by

$$\overline{x}_\alpha = k_0^2 x_\alpha / ck^2 \ , \ \overline{r} = k_0^2 r / ck^2 \ , \ \overline{u} = k_0 u / ck^2 \ . \tag{4.41}$$

Since the solution to the small-scale nonlinear crack problem deduced here involves shocks, along which the displacement gradients suffer jump discontinuities, it is natural to wonder whether it is possible to prove the non-existence of a smoother solution to this problem. We have not been able to supply such a proof; nor have we dealth with questions related to the stability of the solution found.

5. Numerical results for the displacements and stresses. Generalizations of the constitutive assumption. Discussion.

It is clear from (4.1) and the subsequent analysis in Section 4 that

the displacement field of the solution to the pilot problem deduced there is supplied by

$$\bar{u} = \sqrt{2\bar{r}_1}\,\sin\frac{\theta_1}{2} \quad \text{on} \quad \mathcal{E}_* \,, \quad \bar{u} = \frac{f(\theta)}{\bar{r}} \quad \text{on} \quad \mathcal{H}_* \,, \tag{5.1}$$

where $f(\theta)$ is given by (4.2). Here $\mathcal{E}_*$ and $\mathcal{H}_*$ are the final elliptic and hyperbolic domains defined in Section 4 and depicted in Figure 6. Equations (5.1) together with the relations (3.6) between the two pairs of polar coordinates $(\bar{r}_1, \theta_1)$ and $(\bar{r}, \theta)$ may be used to calculate $\bar{u}(\bar{r}, \theta)$. Figure 7 shows curves displaying the angular dependence of $\bar{u}(\bar{r}, \theta)$ for four fixed values of $\bar{r}$. Note that the kink in the curves corresponding to $\bar{r} = 1/4$ and $\bar{r} = \sqrt{2}/2$ is due to the shock. Since the circles $\bar{r} = 7/4$ and $\bar{r} = 9/4$ do not intersect the shock, the remaining two curves in Figure 7 are free of any discontinuity in slope.

From (5.1) follows

$$\lim_{\bar{r}\to 0} \bar{u}(\bar{r}, \theta) = \begin{cases} \sqrt{3} & \text{for} \quad 0 < \theta \le \pi \\ 0 & \text{for} \quad \theta = 0 \\ -\sqrt{3} & \text{for} \quad -\pi \le \theta < 0 \,, \end{cases} \tag{5.2}$$

which accounts for the dashed line in Figure 7. Thus, in first approximation, the material above and below the crack, near its tip, translates rigidly in opposite directions (parallel to the plane of the crack). The displacement discontinuity at the crack tip inherent in (5.2) was mentioned earlier in connection with (4.27).

We proceed now to the determination and discussion of the stresses associated with the solution under consideration. In view of (1.19), (1.22), (1.23), the non-trivial components of the prevailing actual stress field,

referred to the cylindrical coordinates $(r,\theta,z)\equiv(r,\theta,x_3)$, are:

$$\left.\begin{aligned} &\tau_{rz}=2W'(I_1)\frac{\partial u}{\partial r}\,,\quad \tau_{\theta z}=2W'(I_1)\frac{1}{r}\frac{\partial u}{\partial \theta}\,,\quad \tau_{zz}=2W'(I_1)|\nabla u|^2\,,\\ &I_1=3+|\nabla u|^2\,, \end{aligned}\right\}\ (5.3)$$

where W is the elastic potential of the pilot material defined in (1.31). A direct computation relying on the scaling (2.6), the dimensionless displacements (5.1), and involving the polar-coordinate relations (3.6), ultimately yields the results:

$$\left.\begin{aligned} &\tau_{rz}=\frac{\mu}{\sqrt{2\bar{r}_1}}\sin\Big(\theta-\frac{\theta_1}{2}\Big),\quad \tau_{\theta z}=\frac{\mu}{\sqrt{2\bar{r}_1}}\cos\Big(\theta-\frac{\theta_1}{2}\Big)\,,\\ &\tau_{zz}=\frac{\mu}{2\bar{r}_1}\quad \text{on } \mathcal{E}_*\,, \end{aligned}\right\}\ (5.4)$$

which — together with (3.6) — determine the cylindrical components of the Cauchy stress tensor on the elliptic domain $\mathcal{E}_*$ as functions of $\bar{r}$ and θ alone; similarly,

$$\left.\begin{aligned} &\tau_{rz}=-\mu\bar{r}f(\theta)[f^2(\theta)+f'^2(\theta)]^{-3/4}\,,\\ &\tau_{\theta z}=\mu\bar{r}f'(\theta)[f^2(\theta)+f'^2(\theta)]^{-3/4}\,,\\ &\tau_{zz}=\frac{\mu}{\bar{r}}[f^2(\theta)+f'^2(\theta)]^{1/4}\quad \text{on } \mathcal{H}_*\,, \end{aligned}\right\}\ (5.5)$$

with $f(\theta)$ furnished by (4.2).

Figures 8, 9, 10 contain graphs depicting the dependence of the stresses

τ_{rz}, $\tau_{\theta z}$, τ_{zz} upon the polar angle θ for the same four fixed values of $\bar{r}$ employed in Figure 7, except that the results for $\bar{r} = 9/4$ were omitted in Figure 10 in order to avoid an excessively crowded diagram. The curves appropriate to $\bar{r} = 1/4$ and $\bar{r} = \sqrt{2}/2$ in the figures under discussion display finite jump discontinuities at values of θ that are angular polar coordinates of the point of intersection of the corresponding circle $\bar{r} =$ constant with the shock. In contrast, the graphs based on $\bar{r} = 7/4$ reveal merely a discontinuity in slope at the value of θ that corresponds to the intersection between the circles $\mathcal{C}$ and $\bar{r} = 7/4$. At this point of intersection $|\bar{\nabla}\bar{u}| = 1$ and the singular behavior just mentioned can be traced to the kink in the shear-response curve (Figure 3) at $k = 1$. This kink is also responsible for a discontinuity in the curvature of the displacement curve for $\bar{r} = 7/4$ in Figure 7 at the particular value of θ referred to above. Finally, the curves associated with $\bar{r} = 9/4$ in Figures 8, 9 are entirely smooth since this circle lies wholly in the domain of ellipticity of the solution.

If the maximum of $\tau(k)$ occurs at an amount of shear k_0, so that (4.40) hold and the scaling (4.41) is in force, the graphs in Figures 8, 9 represent $\tau_{rz}/\mu k_0$, and $\tau_{\theta z}/\mu k_0$, while those in Figure 10 become plots of $\tau_{zz}/\mu k_0^2$.

Equations (5.4), (5.5) imply that the shear stresses τ_{rz}, $\tau_{\theta z}$ remain bounded as $\bar{r} \to 0$ and tend to zero as the crack-tip is approached from within the hyperbolic domain $\mathcal{H}_*$. This conclusion is consistent with (4.26) and the fact that $\tau(k) \to 0$ as $k \to \infty$ in a simple shear deformation of the special material under consideration. On the other hand,

the axial normal stress τ_{zz}, though bounded in any elliptic neighborhood of the origin $\bar{r}=0$, becomes unbounded as $\bar{r}\to 0$ from within $\mathcal{H}_*$. This singular behavior of τ_{zz} was to be anticipated in view of the last of (1.26), according to which the normal stress τ_{33} induced by a simple shear remains finite as the amount of shear k grows beyond bounds only if $k\tau(k)$ tends to a finite value as $k\to\infty$, whereas $k\tau(k)\sim\mu k^{1/2}$ in this limit for the pilot material[1]. The preceding remark suggests that the singularity of τ_{zz} at the crack-tip would not arise if the second of the relations (1.32) defining the material were suitably modified. Unfortunately, this objective is incompatible with the hodograph scheme we have used to deduce the solution to the problem at hand since the improper integral in (2.17) is no longer convergent when $k\tau(k)=O(1)$ as $k\to\infty$.

Keeping in mind that $|\nabla u|<1$ on $\mathcal{E}_*$ and $|\nabla u|>1$ on $\mathcal{H}_*$, one easily infers from (1.19), (1.23), and (1.31) that

$$W=\frac{1}{2}\tau_{zz} \quad \text{on } \mathcal{E}_*\,, \quad W=2\tau_{zz}-\frac{3\mu}{2} \quad \text{on } \mathcal{H}_*\,. \tag{5.6}$$

The behavior of the strain-energy density associated with the solution being discussed is therefore immediate from that of the axial stress τ_{zz}. In particular, W remains bounded at the crack-tip except when the latter is approached from within $\mathcal{H}_*$.

An analysis strictly parallel to that summarized in the foregoing sections leads to a solution of the analogous small-scale nonlinear crack problem for an incompressible elastic material (of the type characterized by (1.13)) whose response in simple shear obeys

---

[1] See the second of (1.32).

$$\tau(k) = \mu k \quad (0 \le k \le 1) , \quad \tau(k) = \mu k^{-\alpha} \quad (1 \le k < \infty) , \qquad (5.7)$$

in which α is a material constant restricted by

$$0 \le \alpha < 1 . \qquad (5.8)^{1}$$

The constitutive relation (5.7) is evidently a generalization of (1.32) and reduces to (1.32) for $\alpha = 1/2$. The special case $\alpha = 0$ corresponds to a shear response in which the shear stress $\tau(k)$ rises linearly to a value μ at $k = 1$, and remains constant at this value as k increases from unity.

For materials governed by (5.7), (5.8), the differential equation (1.18) again suffers a loss of ellipticity at a solution u and at a point (x_1, x_2), provided $|\nabla u(x_1, x_2)| > 1$.

On applying the hodograph scheme to the small-scale nonlinear crack problem for a material with the shear response (5.7), (5.8), one is once again led to elliptic and hyperbolic solutions of (1.18) on certain subdomains of $\mathfrak{D}$. In fact, Figure 5 remains applicable in the present circumstances, provided the circle C is replaced by one of radius $1/2$ centered at $\bar{x}_1 = \frac{1}{2}(1+\alpha)/(1-\alpha)$, $\bar{x}_2 = 0$, while the angle θ_0 is now determined by $\sin\theta_0 = (1-\alpha)/(1+\alpha)$. Further, the formulas (3.8) and (3.21) for the elliptic and the two hyperbolic solutions at present undergo modifications which will not be spelled out explicitly. As in the special case $\alpha = 1/2$, the elliptic solution can be matched to the appropriate hyperbolic solution across two symmetrically situated shocks, if $0 < \alpha < 1$. Thus Figure 6, which illustrates the elliptic and hyperbolic domains of the final solution for $\alpha = 1/2$, has a qualitatively similar

---

[1] The restriction $\alpha < 1$ assures the convergence of the integrals in (2.17).

counterpart for every value of α in the open interval $(0, 1)$.

The particular case $\alpha = 0$, which is clearly a limiting case of non-elliptic behavior, requires separate comment. In this instance the circle C is centered at $\bar{x}_1 = 1/2$, $\bar{x}_2 = 0$ and thus passes through the origin. When $\alpha = 0$, it turns out, the elliptic solution — analogous to e of (3.8) — can be joined to the non-elliptic solution corresponding to $\overset{+}{h}$ in (3.21) across the entire circle C in such a way that both $\bar{u}$ and its first partial derivatives remain continuous. Hence the final solution thus obtained is free of shocks. It should be mentioned that the finite-crack problem (1.18) to (1.21) for a material obeying (5.7) with $\alpha = 0$ is closely related to a notch-problem for an elastic-perfectly plastic body in anti-plane shear, solved by Hult and McClintock [7], who also employed the hodograph method. In fact, for a notch of zero opening angle (crack) and a sufficiently small loading at infinity, the elastic-plastic interface established in [7] — when referred to the scaling (2.6) — passes over into the circle C that separates the elliptic from the non-elliptic domain in the small-scale nonlinear crack problem corresponding to $\alpha = 0$ in (5.7).

An additional observation pertaining to the special choice of $\alpha = 0$ concerns the solution deduced in [2] to the small-scale crack problem for the limiting elliptic case $n = 1/2$ (see Figure 2) of a power-law material, governed by (1.30). For such a material[1].

[1] See (6.52) in [2] and refer to the scaling (2.6) in the present paper.

$$\lim_{\bar{r}\to 0} \bar{u}(\bar{r},\theta) = \begin{cases} -\mu/\tau_\infty & (-\pi \le \theta < -\pi/2) \\ \mu \sin\theta/\tau_\infty & (-\pi/2 \le \theta \le \pi/2) \\ \mu/\tau_\infty & (\pi/2 \le \theta \le \pi) \ , \end{cases} \tag{5.9}$$

where $\tau_\infty = \mu/\sqrt{2b}$ is the ultimate shear stress. One finds precisely the same result for a simple-shear response (5.7) with $\alpha = 0$, provided τ_∞ in (5.9) is taken to be μ, as is appropriate. This agreement reflects the fact that the behavior of the solution <u>at</u> the crack-tip (as $r \to 0$) in both the limiting elliptic case of a power-law material and the limiting non-elliptic case corresponding to $\alpha = 0$ in (5.7) depends merely on the ultimate shear stress in simple shear.

An alternative modification of (1.32) which is of interest consists in requiring that $\tau(k)$ decline to a positive value τ_∞ — rather than to zero, as in Figure 3. In this event the final solution again involves shocks, but these are no longer tangential to the $\bar{x}_1$-axis at the crack-tip: instead, the two shocks are now found to subtend a positive angle, which depends on the ratio τ_∞/μ.

Another study of crack problems in which the appropriate differential equations of equilibrium are not elliptic is that included in the paper of Hutchinson [8], who investigates the perfectly plastic stress field near the tip of a crack in a thin sheet subject to tension at right angles to the crack. A stress discontinuity arises in the results of the analysis in [8].

In conclusion we remark that the hodograph scheme used in this investigation is no longer available in connection with the physically more important small-scale nonlinear crack problem associated with a crack in a tension field under conditions of plane strain and for a material

capable of sustaining a loss of ellipticity. In preparation for an attack on this much more difficult fourth-order problem, it would be instructive to find an alternative approach to the crack problem treated here that does not rely on the hodograph method.

References

[1] J.K. Knowles, On some inherently nonlinear singular problems in finite elastostatics, Proceedings, Eighth U.S. National Congress of Applied Mechanics, U.C.L.A., June 1978.

[2] J.K. Knowles, The finite anti-plane shear field near the tip of a crack for a class of incompressible elastic solids, International Journal of Fracture, 13 (1977), 5, 611.

[3] I. Sneddon and M. Lowengrub, Crack problems in the classical theory of elasticity, Wiley, New York (1969).

[4] J.R. Rice, Stresses due to a sharp notch in a work-hardening elastic-plastic material loaded by longitudinal shear, Journal of Applied Mechanics, 34 (1967), 287.

[5] J.K. Knowles and Eli Sternberg, On the failure of ellipticity and the emergence of discontinuous deformation gradients in plane finite elastostatics, Journal of Elasticity, 8 (1978), 4, 329.

[6] J.K. Knowles, On the dissipation associated with equilibrium shocks in finite elasticity, Journal of Elasticity, 9 (1979), 2.

[7] J.A.H. Hult and F.A. McClintock, Elastic-plane stress and strain distributions around sharp notches under repeated shear, Proceedings, Ninth International Congress of Applied Mechanics, Brussels, 8 (1956), 51.

[8] J.W. Hutchinson, Plastic stress and strain fields at a crack tip, Journal of the Mechanics and Physics of Solids, 16 (1968), 337.

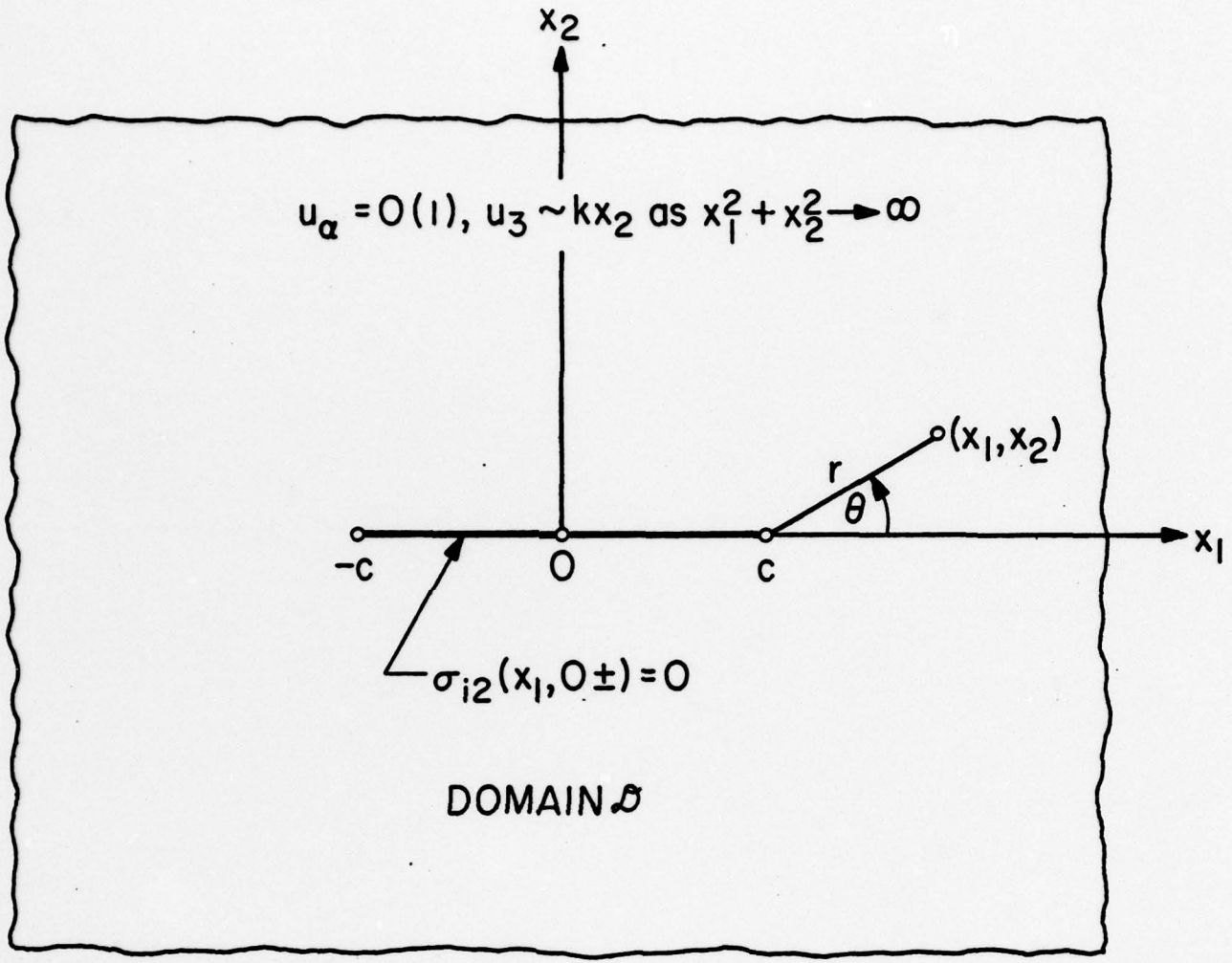

FIGURE 1. CROSS-SECTION OF BODY WITH CRACK AND COORDINATES

$$\tau(k) = \mu\left[1 + \frac{b}{n}k^2\right]^{n-1} k \qquad (0 \le k < \infty)$$

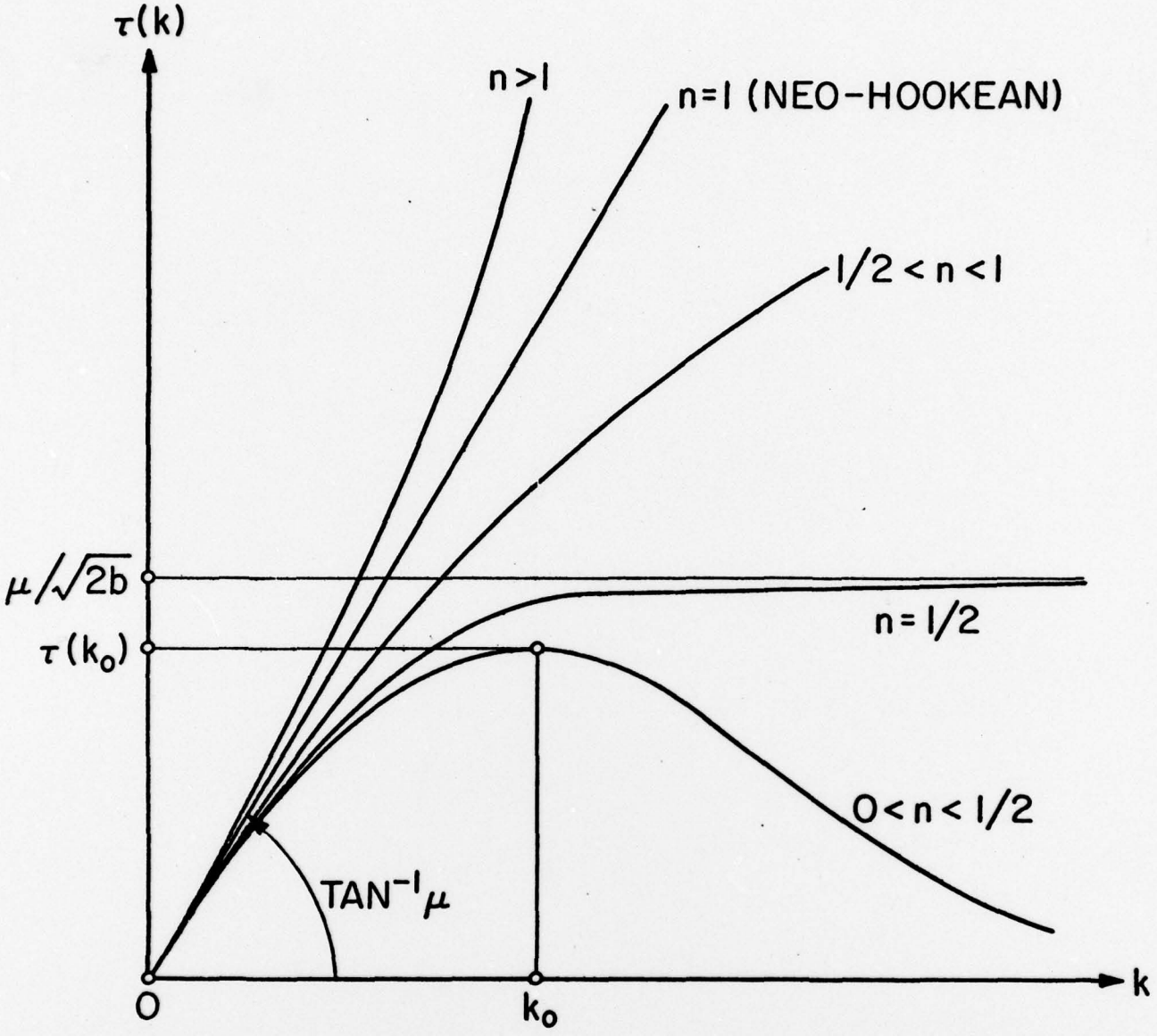

$$k_0 = \sqrt{n/(1-2n)\,b}\,, \quad \tau(k_0) = \mu\left[2(1-n)/(1-2n)\right]^{n-1} k_0$$

FIGURE 2. RESPONSE CURVES IN SIMPLE SHEAR FOR A POWER-LAW MATERIAL

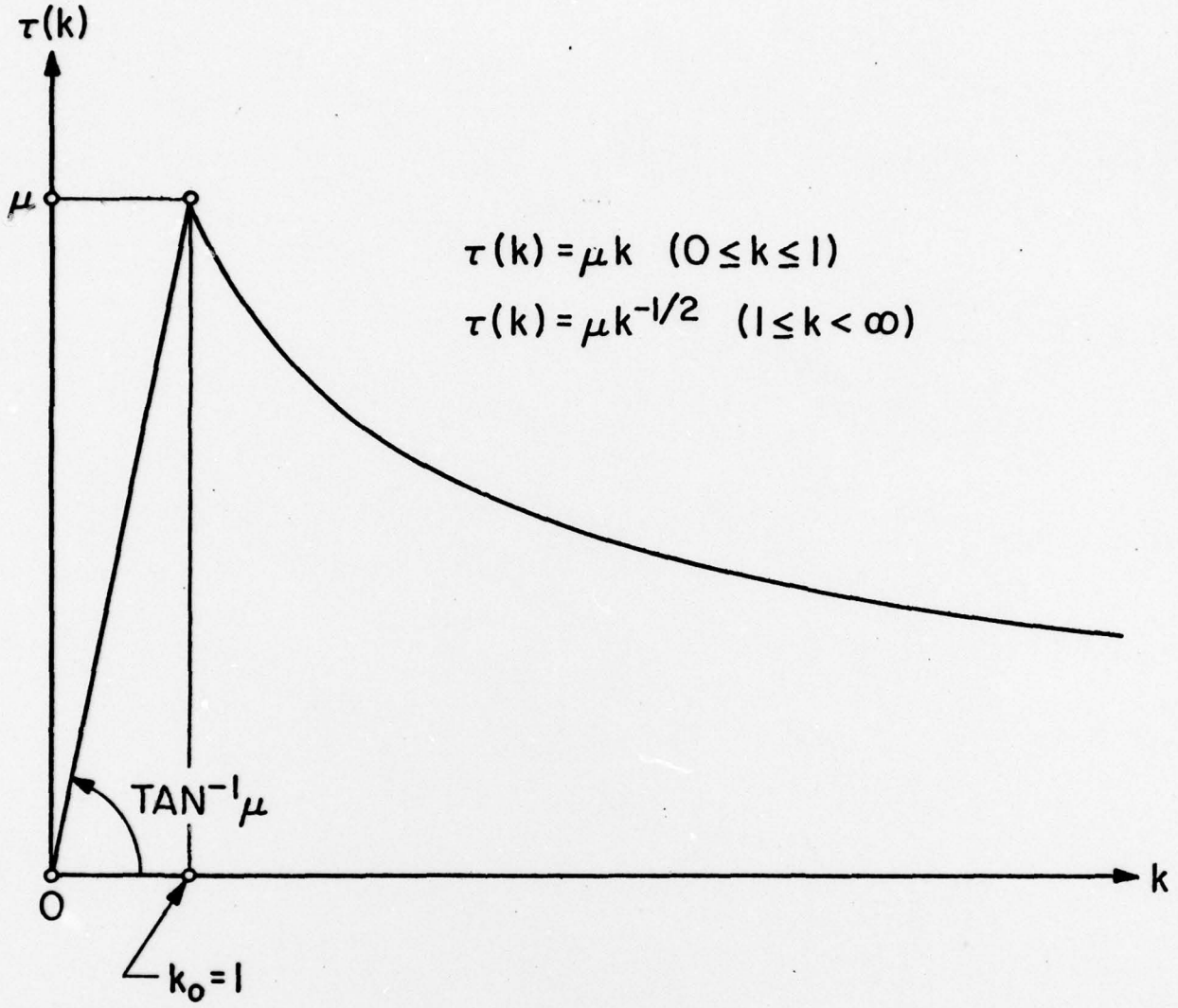

FIGURE 3. RESPONSE CURVE IN SIMPLE SHEAR FOR THE SPECIAL PILOT MATERIAL

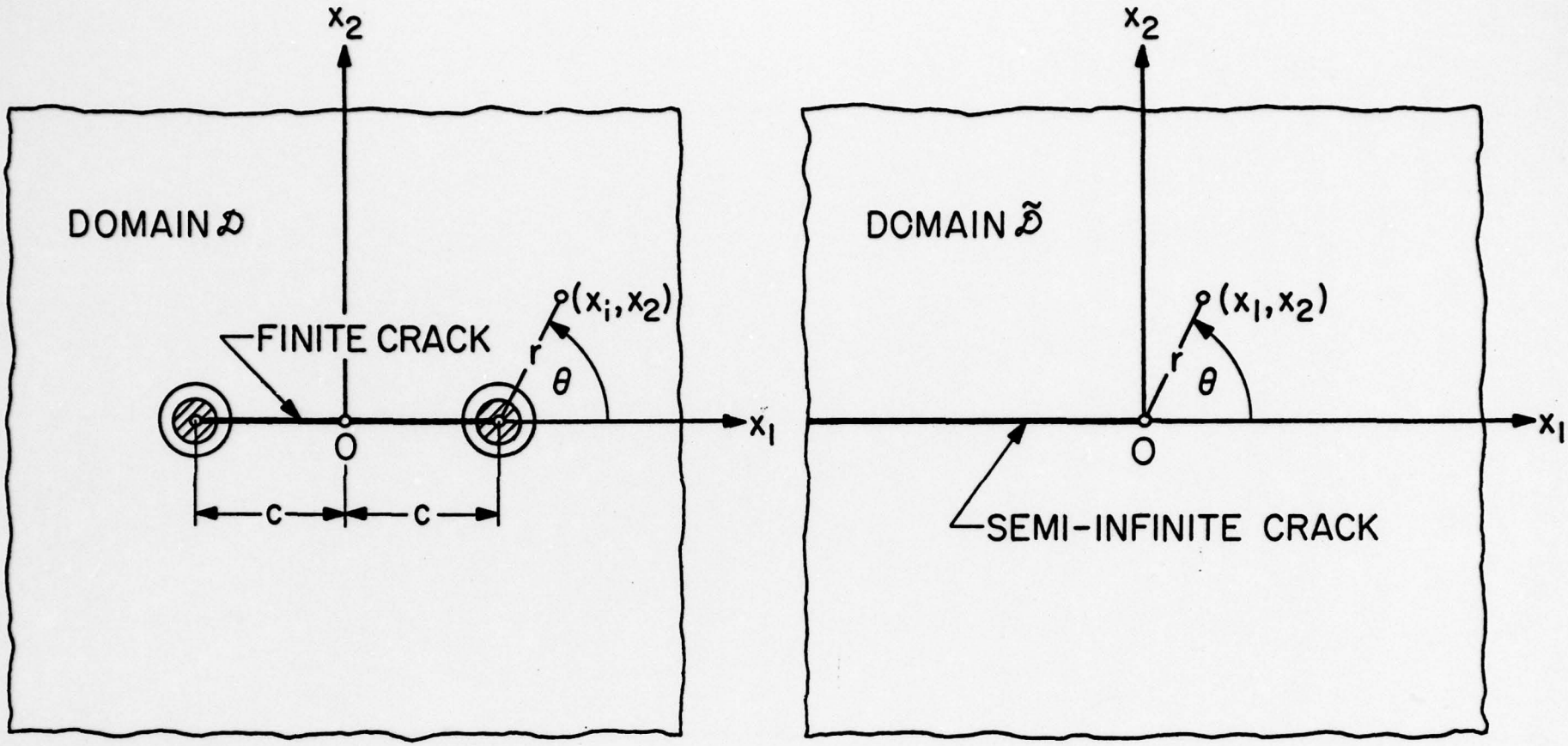

FIGURE 4. CROSS-SECTION OF BODY AND COORDINATES FOR ORIGINAL AND SMALL-SCALE NONLINEAR CRACK PROBLEM

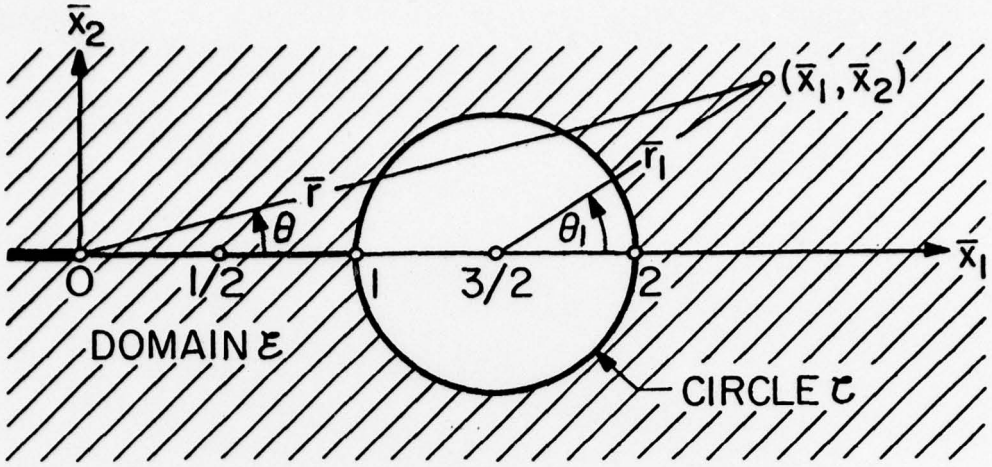

(a) $\bar{u} = e(\bar{x}_1, \bar{x}_2)$ on $\mathcal{E}$ (ELLIPTIC SOLUTION)

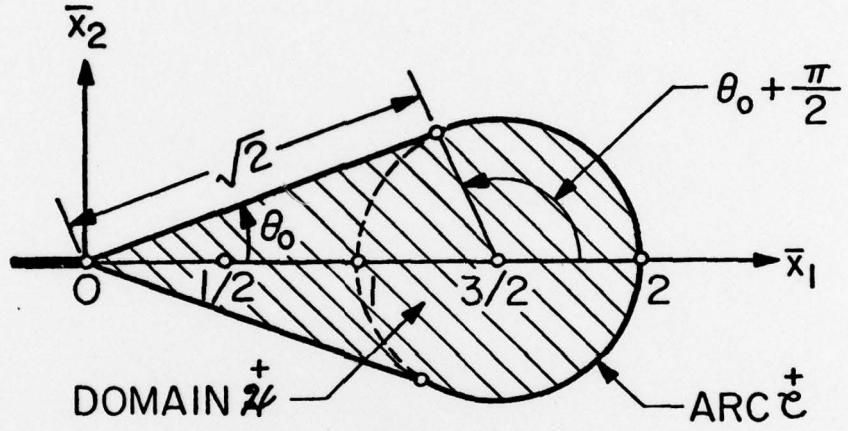

(b) $\bar{u} = \overset{+}{h}(\bar{x}_1, \bar{x}_2)$ on $\mathcal{H}^+$ (HYPERBOLIC SOLUTION)

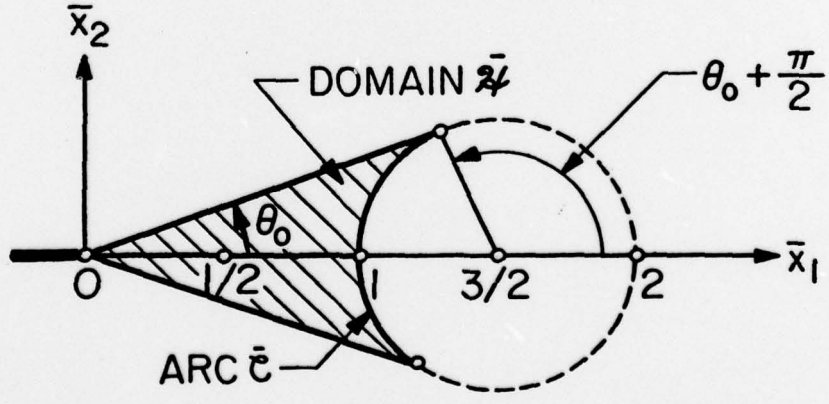

(c) $\bar{u} = \bar{h}(\bar{x}_1, \bar{x}_2)$ on $\mathcal{H}^-$ (HYPERBOLIC SOLUTION)

FIGURE 5. PILOT MATERIAL: ELLIPTIC AND HYPERBOLIC SOLUTIONS

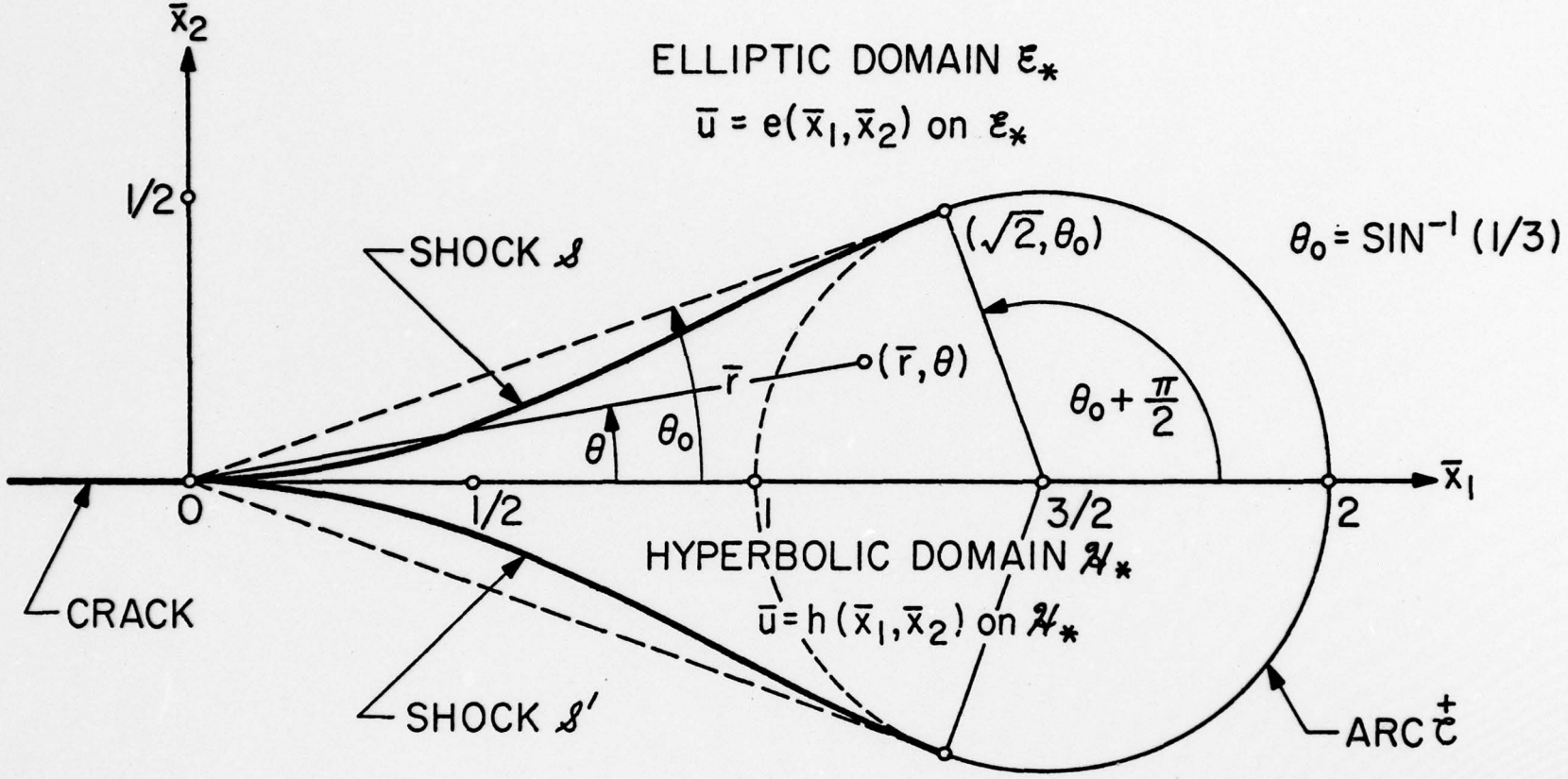

FIGURE 6. SOLUTION OF SMALL-SCALE NONLINEAR CRACK PROBLEM: ELLIPTIC AND HYPERBOLIC DOMAINS

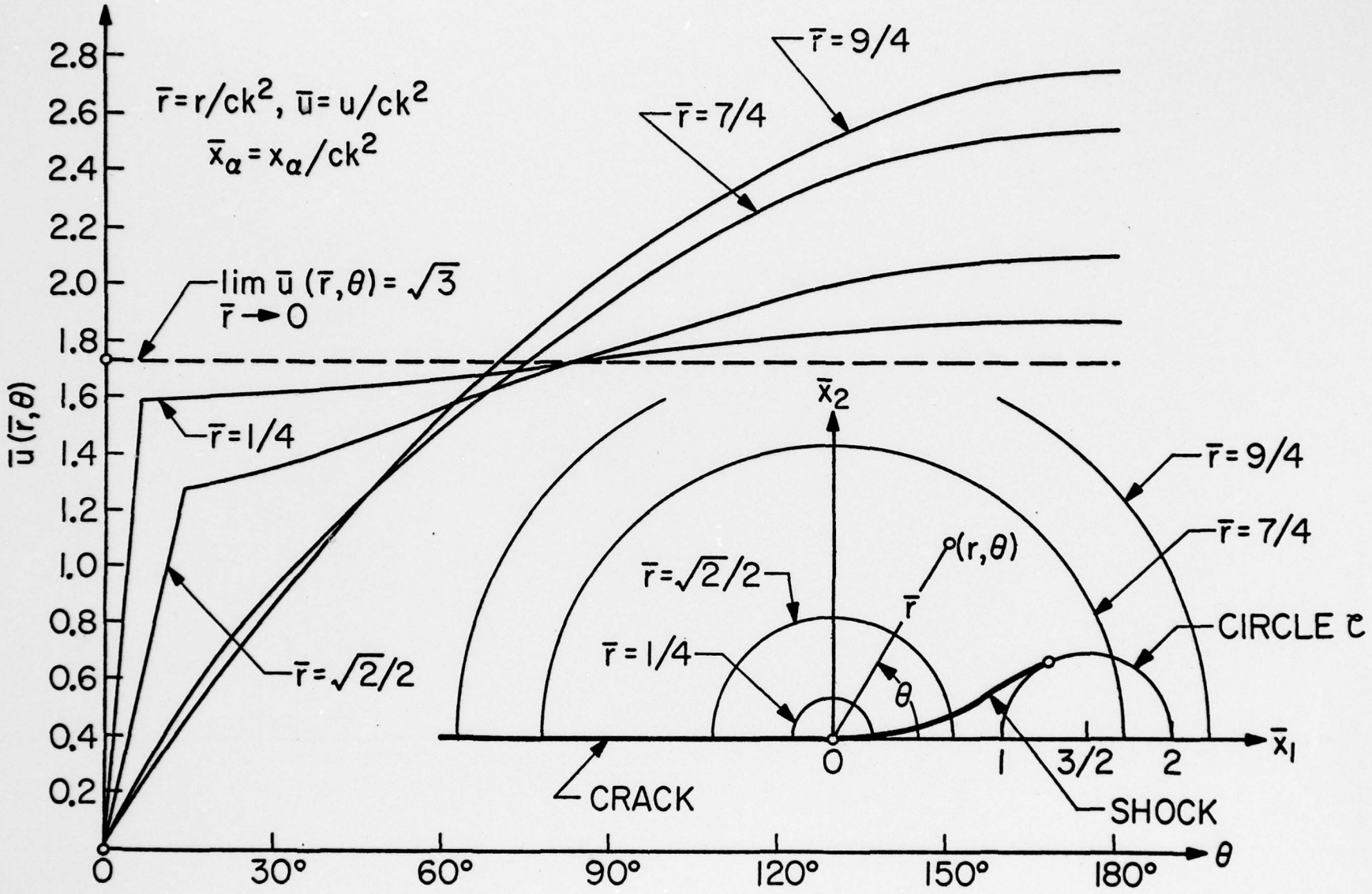

FIGURE 7. ANGULAR DEPENDENCE OF DISPLACEMENT $\bar{u}$

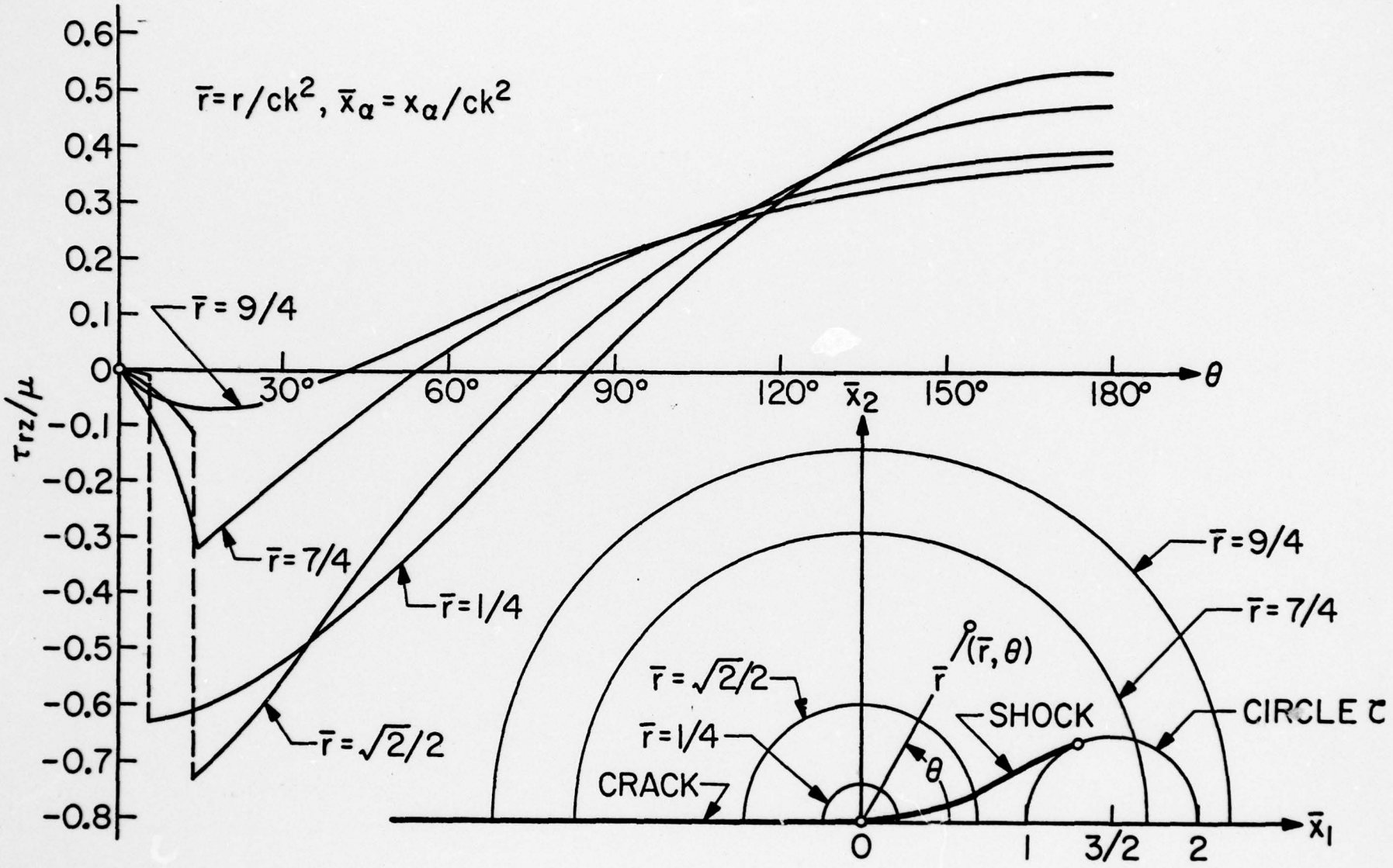

FIGURE 8. ANGULAR DEPENDENCE OF SHEAR STRESS τ_{rz}

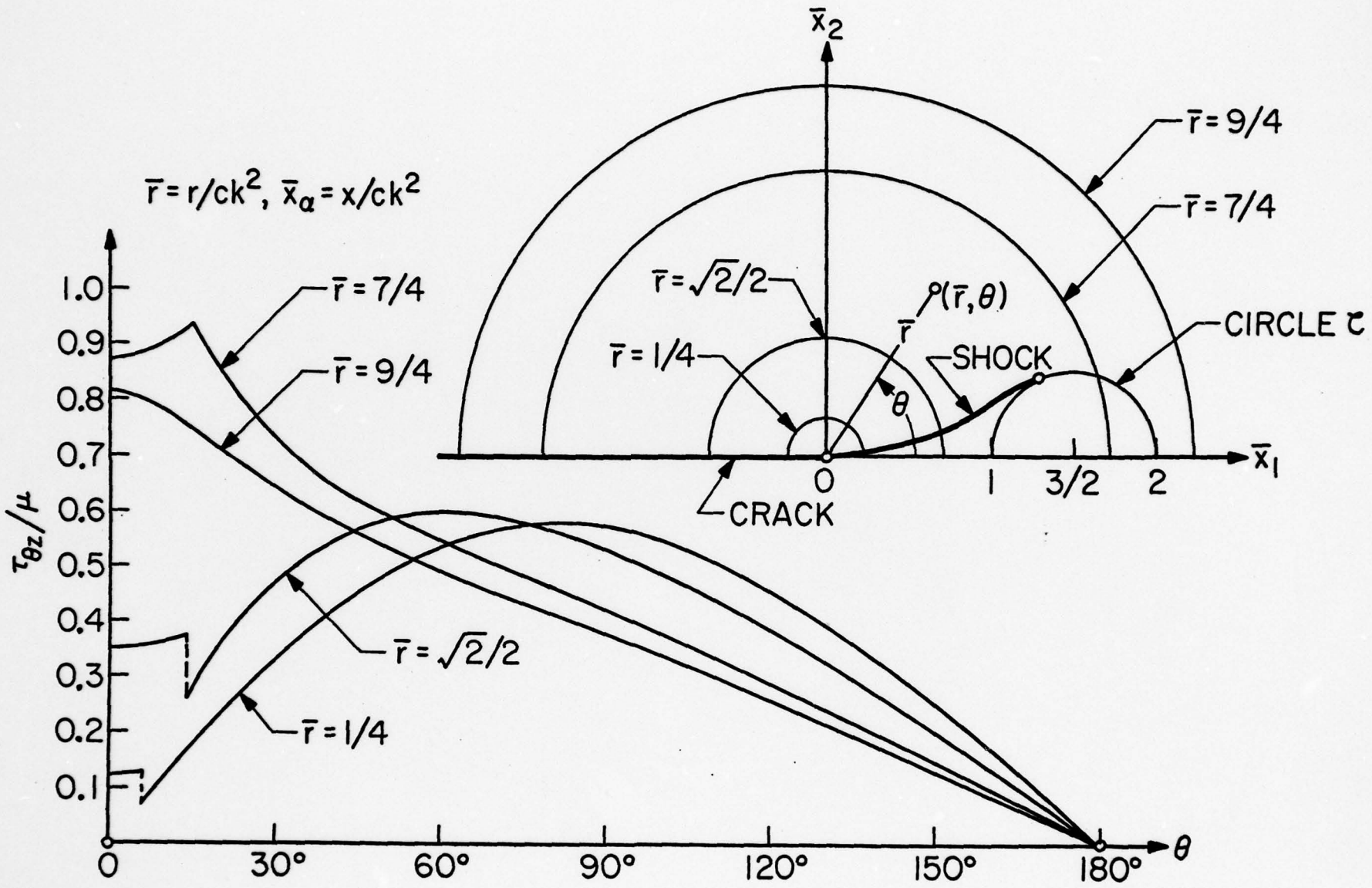

FIGURE 9. ANGULAR DEPENDENCE OF SHEAR STRESS $\tau_{\theta z}$

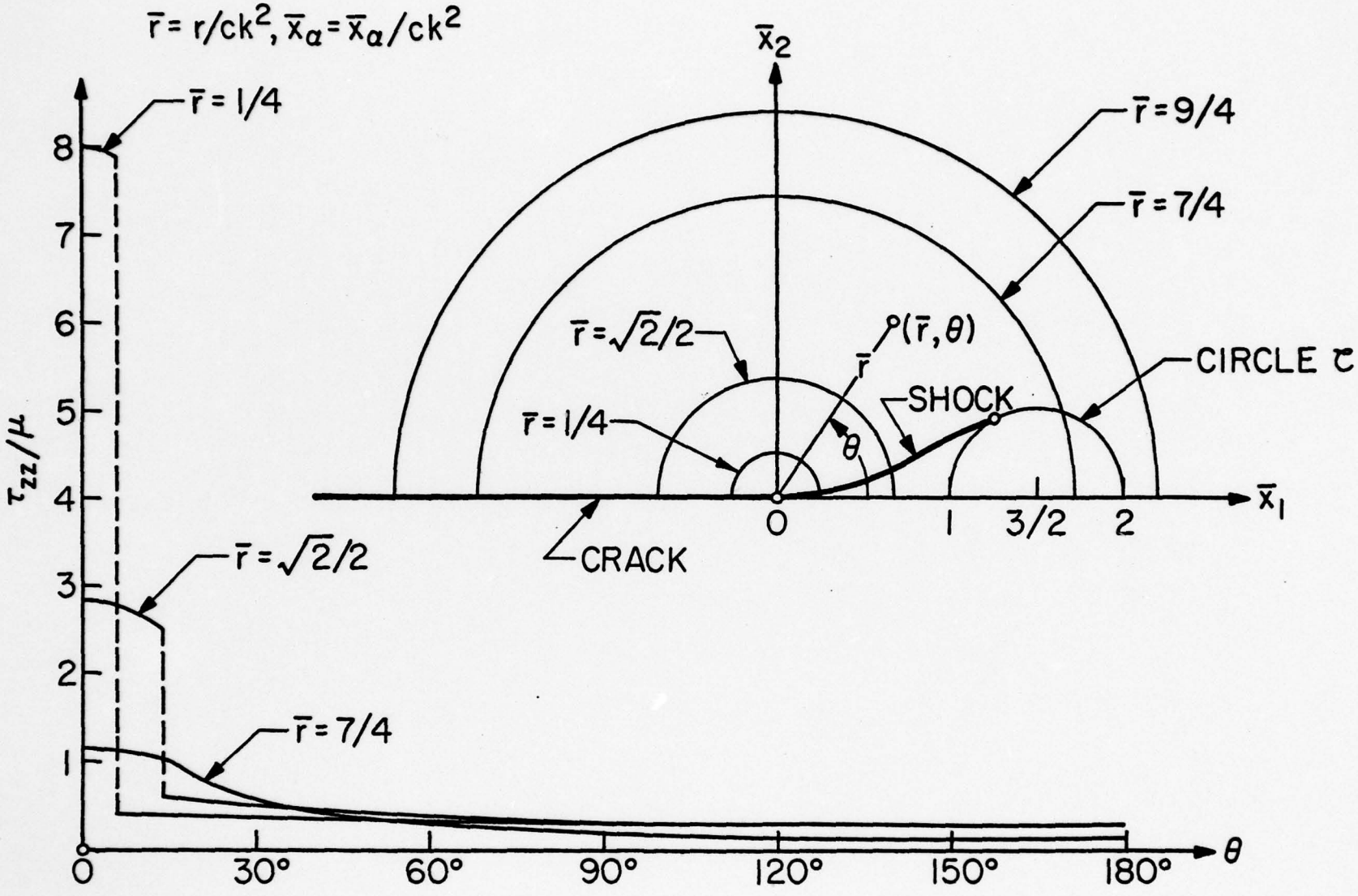

FIGURE 10. ANGULAR DEPENDENCE OF AXIAL STRESS τ_{zz}

Unclassified

Security Classification

DOCUMENT CONTROL DATA - R & D

(Security classification of title, body of abstract and indexing annotation must be entered when the overall report is classified)

1 GINATING ACTIVITY *(Corporate author)*

California Institute of Technology
Pasadena, California 91125

2a. REPORT SECURITY CLASSIFICATION

Unclassified

2b. GROUP

3. REPORT TITLE

Discontinuous deformation gradients near the tip of a crack in finite anti-plane shear: an example

4. DESCRIPTIVE NOTES *(Type of report and inclusive dates)*

Research

5. AUTHOR(S) *(First name, middle initial, last name)*

James K. Knowles and Eli Sternberg

6. REPORT DATE	7a. TOTAL NO. OF PAGES	7b. NO. OF REFS
January 1979	59	8

8a. CONTRACT OR GRANT NO.	9a. ORIGINATOR'S REPORT NUMBER(S)
N00014-75-C-0196	No. 40
b. PROJECT NO.	
c.	9b. OTHER REPORT NO(S) *(Any other numbers that may be assigned this report)*
d.	

10. DISTRIBUTION STATEMENT

Approved for public release; distribution unlimited

11. SUPPLEMENTARY NOTES	12. SPONSORING MILITARY ACTIVITY
	Office of Naval Research Washington, D. C.

13. ABSTRACT

This investigation aims at the elastostatic field near the edges (tips) of a plane crack of finite width in an all-around infinite body, which – at infinity – is subjected to a state of simple shear parallel to the crack faces. The analysis is carried out within the fully nonlinear equilibrium theory of homogeneous and isotropic, incompressible elastic solids. Further, the particular constitutive law employed here gives rise to a loss of ellipticity of the governing displacement equation of equilibrium in the presence of sufficiently severe anti-plane shear deformations.

The study reported in this paper is asymptotic in the sense that the actual crack is replaced by a semi-infinite one, while the far field is required to match the elastostatic field predicted near the crack tips by the linearized theory for a crack of finite width. The ensuing global boundary-value problem thus characterizes the local state of affairs in the vicinity of a crack-tip, provided the amount of shear applied at infinity is suitably small.

An explicit exact solution to this problem, which is deduced with the aid of the hodograph method, exhibits finite shear stresses at the tips of the crack, but involves two symmetrically located lines of displacement-gradient and stress discontinuity issuing from each crack-tip.

DD FORM 1 NOV 65 1473 (PAGE 1)

S/N 0101-807-6801

Unclassified

Security Classification

14. KEY WORDS	LINK A		LINK B		LINK C	
	ROLE	WT	ROLE	WT	ROLE	WT
Elastostatics						
Cracks						
Nonlinear						
Anti-plane shear						